Received: 21 February 2020 | Revised: 19 June 2020 | Accepted: 7 July 2020

DOI: 10.1111/bph.15226

RESEARCH PAPER

Protective effects of Δ^9-tetrahydrocannabinol against enterotoxin-induced acute respiratory distress syndrome are mediated by modulation of microbiota

Amira Mohammed[1] | Hasan K. Alghetaa[1] | Juhua Zhou[1] | Saurabh Chatterjee[2] | Prakash Nagarkatti[1] | Mitzi Nagarkatti[1]

[1]Department of Pathology, Microbiology and Immunology, University of South Carolina School of Medicine, Columbia, South Carolina, USA

[2]Department of Environmental Health Sciences, Arnold School of Public Health, University of South Carolina, Columbia, South Carolina, USA

Correspondence
Mitzi Nagarkatti, PhD, Smart State Endowed Chair of Center for Cancer Drug Discovery, Carolina Distinguished Professor, Chair, Department of Pathology, Microbiology and Immunology, University of South Carolina School of Medicine, 6439 Garners Ferry Road, Columbia, SC 29209, USA.
Email: mitzi.nagarkatti@uscmed.sc.edu

Funding information
Ministry of Higher Education and Scientific Research (MOHESR), Iraq; NIH grants, Grant/Award Numbers: P01AT003961, P20GM103641, R01AI123947, R01AI129788, R01AT006888, R01ES030144

Background and Purpose: Staphylococcal enterotoxin-B (SEB) is one of the most potent bacterial superantigens that exerts profound toxic effects by inducing a cytokine storm. Inhaled SEB can cause acute respiratory distress syndrome (ARDS), which is often fatal and with no effective treatments.

Experimental Approach: Efficacy of Δ^9-tetrahydrocannabinol (THC) was tested in a mouse model of SEB-mediated ARDS, in which lung inflammation, alterations in gut/lung microbiota and production of short-chain fatty acids (SCFAs) was measured. Gene dysregulation of lung epithelial cells was studied by transcriptome arrays. Faecal microbiota transplantation (FMT) was performed to confirm the role of microbiota in suppressing ARDS.

Key Results: While SEB triggered ARDS and 100% mortality in mice, THC protected the mice from fatality. Pyrosequencing analysis revealed that THC caused significant and similar alterations in microbiota in the lungs and gut of mice exposed to SEB. THC significantly increased the abundance of beneficial bacterial species, *Ruminococcus gnavus*, but decreased pathogenic microbiota, *Akkermansia muciniphila*. FMT confirmed that THC-mediated reversal of microbial dysbiosis played crucial role in attenuation of SEB-mediated ARDS. THC treatment caused an increase in SCFA, of which propionic acid was found to inhibit the inflammatory response. Transcriptome array showed that THC up-regulated several genes like lysozyme1 and lysozyme2, β-defensin-2, claudin, zonula-1, occludin-1, Mucin2 and Muc5b while down-regulating β-defensin-1.

Conclusion and Implications: The study demonstrates for the first time that THC attenuates SEB-mediated ARDS and toxicity by altering the microbiota in the lungs and the gut as well as promoting antimicrobial and anti-inflammatory pathways.

KEYWORDS

acute respiratory distress syndrome (ARDS), microbiome, staphylococcal enterotoxin-B (SEB), Δ^9-tetrahydrocannabinol (THC)

Abbreviations: ARDS, acute respiratory distress syndrome; COPD, chronic obstructive pulmonary disease; COVID-19, coronavirus disease 2019; FMT, faecal microbiota transplantation; H&E, haematoxylin and eosin; LDA, linear discriminant analysis; LEfSe, linear discriminant analysis effect size; SCFAs, short-chain fatty acids; SEB, staphylococcal enterotoxin-B; TAC, transcriptome analysis console; THC, Δ9-tetrahydrocannabinol.

1 | INTRODUCTION

Acute respiratory distress syndrome (ARDS) is triggered by a variety of aetiologic agents and staphylococcal enterotoxin-B (SEB) remains one of them. Interestingly, patients who develop the severe form of novel coronavirus disease 2019 (COVID-19) were found to also exhibit ARDS, cytokine storm and respiratory failure (Henry & Lippi, 2020). The incidence of ARDS in the Unites States is 78.9 per 100,000 persons·year^{-1} and the mortality rate is 38.5% (Matthay et al., 2019). With the ongoing COVID-19 pandemic, this incidence is likely to increase further. SEB is capable of inducing fatal ARDS in nonhuman primates following airborne exposure, thereby suggesting that it can also be used as biological warfare agent (Madsen, 2001; Mattix, Hunt, Wilhelmsen, Johnson, & Baze, 1995). The ability of SEB to cause acute ARDS may be related to the fact that it acts as a superantigen by activating a large proportion of T cells expressing certain Vβ-specific T cell receptors, which leads to cytokine storm and consequent injury to various organs, including the lungs (Saeed et al., 2012). It is difficult to treat ARDS and, thus far, there are no pharmacological agents that can protect the host from SEB-mediated toxicity (Nanchal & Truwit, 2018; Rubenfeld & Herridge, 2007). Recent studies from our laboratory demonstrated that exposure to two small doses of SEB in C3H mice can trigger acute ARDS, which if left untreated, leads to 100% mortality (Alghetaa et al., 2018; Mohammed et al., 2020). Interestingly, we were able to show that administration of **Δ^9-tetrahydrocannabinol (THC)** prior to SEB challenge e prevents such toxicity and mortality by suppressing the cytokine storm and enhancing immunosuppressive cytokines such as **IL-10** as well as induction of regulatory T cells (Tregs; Rao, Nagarkatti, & Nagarkatti, 2015).

Currently, there are no FDA-approved drugs to treat ARDS. Pharmacological agents such as corticosteroids and neuromuscular blocking agents may be beneficial for ARDS patients, but the mortality rate remains high (Mokra, Mikolka, Kosutova, & Mokry, 2019). THC is a cannabinoid component found in marijuana (*Cannabis sativa* L.). THC acts through cannabinoid receptors, **CB_1** and **CB_2**, that are expressed on immune cells (Mohammed et al., 2020; Nagarkatti, Pandey, Rieder, Hegde, & Nagarkatti, 2009). THC is well characterized to exhibit anti-inflammatory properties. THC uses multiple pathways to mediate immunosuppression including (1) induction of regulatory T cells (Tregs) and myeloid-derived suppresser cells (MDSCs; Hegde, Nagarkatti, & Nagarkatti, 2010; Pandey, Hegde, Nagarkatti, & Nagarkatti, 2011; Sido, Nagarkatti, & Nagarkatti, 2015), (2) apoptosis in activated T cells and dendritic cells (McKallip, Lombard, Martin, Nagarkatti, & Nagarkatti, 2002; Rieder, Chauhan, Singh, Nagarkatti, & Nagarkatti, 2010), (3) switch from Th1 to Th2 differentiation (Yang et al., 2014) and (4) inhibition of cytokine production by up-regulation of suppressor of cytokine signalling 1, a negative regulator of **IFN-γ** (Sido, Jackson, Nagarkatti, & Nagarkatti, 2016). We have also shown that THC triggers epigenetic changes including alterations in the expression of miRNA (Al-Ghezi, Miranda, Nagarkatti, & Nagarkatti, 2019) and histone modifications (Yang et al., 2014). For example, in SEB-induced mouse model of ARDS, our previous studies showed that THC could modulate the expression of miR17–92 cluster and suppress SEB-induced ARDS (Rao et al., 2015).

Recent studies have shown that gut microbiome may play a critical role in disease pathogenesis involving other organs besides the gut (Das & Nair, 2019). This stems from the fact that the gut microbiota produce short-chain fatty acids that can travel systemically and cause immunomodulatory changes at distant sites (Dopkins, Nagarkatti, & Nagarkatti, 2018). A recent study from our laboratory suggested that cannabinoids can trigger dysbiosis that is beneficial to the host. For example, we found that THC and **cannabidiol** can reverse the dysbiosis triggered in the gut during an experimental multiple sclerosis model and that the efficacy of these cannabinoids to attenuate this autoimmune disease depended on their effect on microbiota (Al-Ghezi, Busbee, Alghetaa, Nagarkatti, & Nagarkatti, 2019).

While SEB is well characterized to cause ARDS through induction of inflammatory cytokines and infiltration of mononuclear cells into the lungs, there are no studies to test if SEB can also alter the microbiota in the lungs and the gut and how such dysbiosis can impact the lung inflammation and ARDS. Additionally, while we have shown previously that THC can attenuate SEB-mediated ARDS, whether this results from THC-mediated dysbiosis in the lungs has not been previously investigated.

In this study, we comprehensively investigated the effects of THC treatment on lung and gut microbiome, induction of antimicrobial enzymes and peptides and nature of immune response induced during SEB-induced ARDS mice. Excitingly, our results

What is already known

- Cannabinoids exhibit anti-inflammatory properties.
- Bacterial enterotoxins elicit acute respiratory distress syndrome (ARDS) that is lethal and difficult to treat.

What this study adds

- THC administered after exposure to an enterotoxin can prevent mortality by suppressing inflammation in lungs.
- THC-mediated attenuation of ARDS results from alterations in microbiota and their products in lungs.

What is the clinical significance

- Cannabinoids may be highly effective in treating ARDS which is also seen in COVID-19 patients.
- Modulation of microbiota or their products e.g. short-chain fatty acids, may help in treating ARDS.

showed that SEB caused marked but similar alterations in microbiota found in the gut and lungs in ARDS-induced mice. Moreover, THC treatment led to reversal of such dysbiosis and importantly, faecal microbiota transplantation experiments showed that the ability of THC to attenuate SEB-mediated ARDS resulted from THC-induced alterations in the microbiota. The current study provides evidence for the first time that the lung and gut microbiota may play a critical role in SEB-mediated pathogenesis of ARDS and thus agents that can reverse such dysbiosis may be helpful to treat ARDS.

2 | METHODS

2.1 | Mice

C3H/HeJ (RRID:IMSR_JAX:000659) mice were obtained from the Jackson Laboratory (Bar Harbor, Maine). Female mice, 8–10 weeks of age, were used throughout the studies. Animals were housed in specific pathogen-free conditions and all experiments were approved by Institutional Animal Care and Use Committee (AUP2363). Animal studies are reported in compliance with the ARRIVE guidelines (Percie du Sert et al., 2020) and with the recommendations made by the *British Journal of Pharmacology* (Lilley et al., 2020).

2.2 | Animals grouping and housing

All delivered mice were kept for 1 week as acclimatization period prior to performing any experiments. Animals were housed in maximum of five mice per cage under 12-h light/12-h dark cycle at a temperature of ~18–23°C and 40–60% humidity. Food and water were available ad libitum. To minimize the microbiome variations from cage/rack to cage/rack due to managerial and housekeeping effects, experimental mice were selected randomly from different cages to house them in one new cage with a maximum number of five mice per cage. Then each cage was blindly assigned for different treatments or kept as control group according to the experimental design. The person who carried out the experiments was not blinded because of injection of SEB, vehicle and THC at different times, but most data analysis and experiments were blinded to avoid any bias.

2.3 | Induction of ARDS

Staphylococcal enterotoxin-B (SEB) was purchased from Toxin Technologies (Sarasota, FL, USA) and used in the induction of ARDS as a "dual dose" as described previously (Huzella, Buckley, Alves, Stiles, & Krakauer, 2009). Briefly, 25 μl of SEB at a concentration of 0.2 $\mu g \cdot \mu l^{-1}$ (5 μg total per mouse) was intranasally administered into each C3H/HeJ mouse with a micropipette. After 2 h, the same mouse received an intraperitoneal injection of 100 μl of SEB at a concentration of 0.02 $\mu g \cdot \mu l^{-1}$ (2 μg total per mouse).

2.4 | Treatment of THC

THC was dissolved in ethanol and then diluted in 1× PBS. Each mouse was treated intraperitoneally with THC that was given at 20 $mg \cdot kg^{-1}$, i.p. immediately after first SEB exposure. Second and third doses of THC were given i.p. at 10 $mg \cdot kg^{-1}$ after 24 and 48 h after the first dose of THC. Disease progress in mice was assessed by the evaluation of cytokine levels in the serum and histopathology on the third day after SEB administration. Faecal contents were collected for 16S rRNA pyrosequencing for microbiome metagenomics analysis and short-chain fatty acids production evaluation.

2.5 | Collection of lung tissues

At the endpoint of the experiment, all mice were euthanized by exposing them to overdose of isoflurane and then the lung tissues were removed for further analysis. Small portions of lung tissues were used in the isolation of bacterial DNA and histopathology, as described (Elliott, Nagarkatti, & Nagarkatti, 2016). Lung tissues were also smashed using a Stomacher 80 Biomaster lab blender (Metrohm USA, Riverview, FL) in 10 ml of RPMI-1640 medium, lysed with Red Blood Lysing Buffer (Sigma-Aldrich, St. Louis, MO, USA) to remove red blood cells, washed with PBS, filtered and resuspended in PBS supplemented with 5% FCS. Then lung-associated mononuclear cells were isolated from lung cell suspensions in Ficoll-Histopaque®-1077 (Sigma-Aldrich) at a 1:1 ratio under 350 g of centrifugation for 30 min, as described (Alghetaa et al., 2018). The lung-associated mononuclear cells were stored immediately in TRIzol reagent at −80°C freezer for RNA sequencing. The portions of lung-associated mononuclear cells were used in the measurement of proton efflux rate. Also, broncho-alveolar lavage fluid (BALF) was collected from these euthanized mice according to the procedure described by Alghetaa et al. (2018).

2.6 | ELISA of cytokines

Serum samples were used in the measurement of cytokines including **TNF-α**, IFN-γ, chemokine (C–C motif) ligand 5 (**CCL5**), monocyte chemoattractant protein-1 (**MCP-1/CCL2**) and **TGF-β**, by means of ELISA according to the manufacturer's protocol. All ELISA kits of mouse cytokines were purchased from BioLegend (San Diego, CA, USA).

2.7 | Histopathology of lung tissues

Lung tissues from mice were fixed in 4% paraformaldehyde solution, dehydrated in alcohol and embedded in paraffin for microtome section preparation. The sections with 5 μm thick were stained with haematoxylin and eosin (H&E) and examined for inflammatory cell infiltrates under Leica fluorescence microscope system.

2.8 | Immunofluorescence staining of lung tissues

Immunofluorescence staining of lung tissues was carried out as described earlier (Alharris et al., 2018; Sarkar et al., 2019). Briefly, the sections of lung tissues were deparaffinized according to the standard protocol and treated with the antigen-retrieval solution from Abcam (Cambridge, MA) for antigen retrieval. The sections were washed with PBS twice, permeabilized with 0.01% Triton X-100 (Sigma) for 15 min, washed three times with PBS, and then incubated overnight at 4°C with the primary antibody from Abcam diluted in PBS containing 1% FBS. Next, the sections were washed with PBS three times, incubated with anti-mouse secondary antibody Goat Anti-Mouse IgG H&L (Alexa Fluor® 488) antibody (RRID:AB_2576208) for MUC5AC (1:200, Abcam, Cat# ab3649; RRID:AB_2146844) and Goat Anti-Mouse IgG H&L (Alexa Fluor® 647) antibody (RRID:AB_2811129) for MUC5b (1:500, ab77995; RRID:AB_2146987), diluted in PBS with 1% FBS for 1 h at 37°C and washed three times with PBS. The sections were then stained with DAPI to display the nuclei in the cells, washed three times with PBS and finally mounted with Antifade Mounting Medium from Vector Labs (Burlingame, CA). The sections were visualized and photographed using Leica fluorescence microscope system. The corrected total cell fluorescence for cells in the lung tissues was calculated using ImageJ (RRID:SCR_003070) software from NIH (Bethesda, MD). Mucin 5AC (MUC5AC) was stained using anti-MUC5AC mouse antibody, while MUC5b was stained using anti-MUC5b mouse antibody. The corrected total cell fluorescence was measured using ImageJ software. Corrected total cell fluorescence = Integrated density − (Area of selected cell × Mean fluorescence of background readings). The Immuno-related procedures used comply with the recommendations made by the *British Journal of Pharmacology*.

2.9 | Flow cytometry of immune cells

Lung samples were collected from individual mice and treated with lysis buffer to remove red blood cells. Single-cell suspensions were prepared and incubated with Fc block (anti-**CD16/32**) from BD Biosciences (San Jose, CA) for 15 min at 4°C to block Fc receptors. After washing with FACS staining buffer (PBS with 1% BSA), single-cell suspensions were stained. To determine the phenotypical characteristics of the infiltrating cells, mononuclear cells were stained with the fluorescent-conjugated antibodies phycoerythrin (PE)-conjugated anti-**CD4** (clone: RM4-4, RRID:AB_313690), BV510-conjugated anti-Gr-1 (clone: RB6-8C5, RRID:AB_2562215), Alexa Fluor 700-conjugated anti-CD11b (clone: M1/70, RRID:AB_493705), BV421-conjugated anti-CD3 (clone: 17A2, RRID:AB_10900227), Alexa Fluor 647-conjugated anti-CD8 (clone: 53-6.7, RRID: AB_493424) and P/Dazzle-conjugated anti-NK1.1 (clone: PK 136, RRID:AB_2564219) from BioLegend for 30 min. The cells were washed two times with FACS staining buffer, resuspended in BD Cytofix/Cytoperm solution and incubated for 20 min. The cells were washed again two times with BD perm/wash solution intracellular staining of Foxp3 and were carried out using BioLegend's Foxp3 Fix/Perm buffer set following the manufacturer's instructions and using IFN-γ APC (clone XMG 1.2, RRID:AB_315403) from BioLegend for 30 min at 4°C in the dark for intracellular cytokine staining. Cells were washed thoroughly with FACS staining buffer and analysed by BD FACSCelesta flow cytometer and DIVA software.

2.10 | Analysis of transcriptome

Lung epithelial cells were prepared according to the procedures described by the other investigators (Chapman et al., 2011; Vaughan et al., 2015). Briefly, lung samples were collected from individual mice and injected with 1 ml of dispase down trachea. Then the trachea was tied using string and the lungs were rinsed with cold PBS. To minimize contamination with bronchial epithelial cells, each lung lobe was cut from the main stem bronchi. The proximal-most ¼ of each lobe surrounding the bronchi was cut and the lobes were placed into a 50-ml tube containing dispase and rocked at room temperature for 45 min. Cell isolation was carried out as follows. In a cell culture hood, 10 ml of sort buffer and 50 $U \cdot ml^{-1}$ of DNAse were added to dissociate the lung tissue. The content was passed through 100-, 70- and 40-μm cell strainers over 50-ml tubes. The filtered suspension was transferred into a 15-ml tube and spun for 5 min at 550 g at 4°C to pellet cells. The cells were resuspended in 10 ml of sort buffer and left to recover shaking for at least 1 h at 37°C. Then to increase the lung epithelial cells enrichment and get rid of any non-epithelial cells, CD326 antibody conjugated with PE Fluor chrome (clone: G8.8, RRID: AB_1134172) (BioLegend) was used to positively purify the cell suspension by using magnetic microbeads (Stem Cell Technology, USA) according to the manufacturer's protocol. The cells were kept in Qiazol (Qiagen, Valencia, CA, USA) for 5 min at room temperature to break down the cellular membrane and used in the isolation of total RNA samples according to the manufacturer's manual of miRNeasy Mini Kit (Qiagen). GeneChip WT plus reagent kit (Affymetrix, Santa Clara, CA) was used in the synthesis of fragmented single-stranded cDNAs (ss-cDNAs) from the total RNA samples with primers containing a T7 promoter sequence. The second-strand cDNAs were prepared from the first-stranded cDNAs using PCR. Next, the cRNAs were synthesized and amplified using T7 RNA polymerase according to Eberwine method (Borner, Smida, Hollt, Schraven, & Kraus, 2009; Van Gelder et al., 1990) and purified by the magnetic microbeads (Affymetrix). The purified cRNAs were used to synthesize the second cycle of ss-cDNAs using the second-cycle primers. Then the second cycle of ss-cDNAs was purified by the microbeads and fragmented by uracil-DNA glycosylase and apurinic/apyrimidinic endonuclease 1 at the unnatural dUTP residues. The fragmented ss-cDNAs were labelled with the labelling master mix and hybridized in the GeneChip Hybridization Oven 645 (Affymetrix) at 45°C for 16 h with rotation at speed of 60 rpm using Clariom D chip (Affymetrix). The hybridization chips were washed and stained at room temperature for 2 h using GeneChip Fluidics Station 450 (Affymetrix). Lastly, the chips were analysed using GeneChip Scanner (Affymetrix) to profile the mouse

transcriptome arrays. Transcriptome analysis console (TAC) was used to analyse and interpret the mouse transcriptome array data for specific gene expression profiles. The dysregulation of several specific genes was validated by real-time PCR.

2.11 | Quantification of the genes with real-rime PCR

To validate the genes of interest, cDNA was prepared from isolated RNA with miScript II RT Kit (Qiagen) and qRT-PCR (Bio-Rad, USA) was used to determine expression levels. The data were expressed as fold change by comparing the experimental groups to naïve controls (fold mean of the controls) and considering the naïve expression as 1. PCR reactions were performed using miScript II Primer Assay (Qiagen). To quantitate gene expression, custom primers were designed and purchased from Integrated DNA Technologies (IDT) and SSO Advanced SYBR® Green (Bio-Rad) was used for the subsequent PCR reactions. The following custom primers were used: mRNA, forward 5′-3′ and reverse 5′-3′; lysozyme1 (Lyz1), 5′-GAGACCG-AAGCACCGACTATG-3′ and 5′-CGGTTTTGACATTGTGTTCG-3′; lysozyme2 (Lyz2), 5′-ATGGAATGGCTGGCTACTATGG-3′ and 5′-ACCAGTATCGGCTATTGATCTGA-3′; β-defensin-1 (Defb1), 5′-AGGTGTTGGCATTCTCACAAG-3′ and 5′-GCTTATCTGGTTTACAG-GTTCCC-3′; β-defensin-2 (Defb2), 5′-TCCTGGTTGACGAGACCACA-3′ and 5′-AGGCATTTCTGCATAACCCCT-3′; Mucin2 (Muc2), 5′-TCCAGGTCTCGACATTAGCAG-3′ and 5′-GTGCTGAGAGTTTGCG-TGTCT-3′; Muc5b, 5′-GTGGCCTTGCTCATGGTGT-3′ and 5′-GGAC-GAAGGTGACATGCCT-3′; claudin 18, 5′-ATGGGCTTAGTCTT-CCGAACG-3′ and 5′-CTTCCAGTGCGGCAAGTAGTT-3′; zonula-1 (Zo-1), 5′-CTCCAGAGCACCGAGAGCTA-3′ and 5′-GGCGTTTGCG-AAGTTCTTCAT-3′; and occludin, 5′-TTGAAAGTCCACCTCCTT-ACAGA-3′ and 5′-CCGGATAAAAAGAGTACGCTGG-3′.

2.12 | Pyrosequencing of microbiome

Lung tissues and colon samples were used in pyrosequencing for microbiome analysis, as described previously (Cox et al., 2017). Briefly, the extraction of genomic DNA from lung tissues and colon samples was carried out using the QIAamp DNA Stool Mini Kit (Qiagen) according to the manufacturer's instruction. The DNA concentrations were determined using a NanoDrop ND-1000 spectrophotometer (Thermo Fisher Scientific, Waltham, MA) and stored at −20°C for further analysis. The 16S rRNA V3-V4 hypervariable regions of bacterial DNA were amplified by PCR using the 16S V3-314F forward primer 5′-TCGTCGGCAGCGTCAGATGTGTATAAGAGACAGCCTAC-GGGNGGCWGCAG-3′ and V4-805R reverse primer 5′-GTCTCGTGGGCTCGGAGATGTGTATAAGAGACAGGACTACHV-GGGTATCTAA TCC-3′ at 95°C for 3 min and 25 cycles of 95°C 30 s, 55°C 30 s and 72°C 30 s, and a final extension at 72°C for 5 min (Tauxe et al., 2015). Illumina (San Diego, CA) adapter overhang nucleotide sequences were added and the reactions were cleaned up with Agencourt AMPure XP beads. Then both dual indices and Illumina sequencing adapters were attached by PCR using the reaction mixture of 5 μl of amplicon PCR product DNA, 5 μl of Illumina Nextera XT Index Primer 1 (N7xx), 5 μl of Nextera XT Index Primer 2 (S5xx), 25 μl of 2× KAPA HiFi Hot Start Ready Mix and 10 μl of PCR-grade water at 95°C for 3 min and 8 cycles of 95°C 30 s, 55°C 30 s and 72°C 30 s and a final extension at 72°C for 5 min. Next, the constructed 16S metagenomic libraries were purified with Agencourt AMPure XP beads and quantified with Quant-iT PicoGreen. Library quality and average size distribution were determined with the Agilent Technologies 2100 Bioanalyzer. Amplicons in the libraries were subject to pyrosequencing using the MiSeq Reagent Kit V3 in the Illumina MiSeq System. Sequenced data collected from the Illumina MiSeq System were analysed by means of the online 16S analysis software from NIH, known as Nephele (RRID: SCR_016595) (https://nephele.niaid.nih.gov/) to determine microbial compositions (Weber et al., 2018).

2.13 | Faecal microbiota transplantation

Colonic materials were collected from eight donor mice in each group and used in faecal microbiota transplantation, as described (Al-Ghezi, Busbee, et al., 2019). Briefly, donor mice that were euthanized with an overdose of isoflurane were moved into an anaerobic chamber where the abdominal wall was opened and the colon tissues were collected. The colonic content was then scraped and suspended in sterile PBS before being filtered and weighed and then loaded into tuberculin syringe attached to an oral gavage tube for transfer. Recipient mice were extensively treated with different antibiotics (i.e. antibiotics cocktail cocktail) for 4 weeks in drinking water to ensure the complete depletion of endogenous microbiome as described previously (Chevalier et al., 2015; Grivennikov et al., 2012). The antibiotics cocktail was composed of 250 $mg \cdot ml^{-1}$ of bacitracin, 170 $\mu g \cdot ml^{-1}$ of gentamycin, 125 $\mu g \cdot ml^{-1}$ of ciprofloxacin, 100 $\mu g \cdot ml^{-1}$ of neomycin, 100 $\mu g \cdot ml^{-1}$ of metronidazole, 100 $\mu g \cdot ml^{-1}$ of ceftazidime, 100 $U \cdot ml^{-1}$ of penicillin, 50 $\mu g \cdot ml^{-1}$ of streptomycin and 50 $\mu g \cdot ml^{-1}$ of vancomycin. This cocktail was replaced with freshly prepared cocktail every 5 days during the antibiotic treatment period. The complete depletion of endogenous microbiome in the gut of recipient mice was confirmed by PCR validation and bacteriological culture. Faecal pellets were collected aseptically under anaerobic conditions by enriching the chamber environment with special gas mixture (Praxair, Columbia, SC) from all recipient mice 3 days before the end of antibiotics treatment for the confirmation of complete depletion of endogenous microbiome in the gut. Recipient mice received oral administration of normalized amount of faecal materials in PBS from each group of mice twice using tuberculin syringes in the anaerobic chamber to protect collected gut anaerobic bacteria from free oxygen during faecal microbiota transplantation. Immediately after faecal microbiota transplantation, the recipient mice received the first intranasal administration of SEB. After 24 h, the recipient mice received the second intraperitoneal injection of SEB, as described above. Disease progress in mice was assessed by the evaluation of mouse survival for 30 days. On the third day after SEB

administration, five mice from each group were killed for the preparation of lung-associated mononuclear cells for flow cytometry analysis and for the collection of colon contents for 16S rRNA pyrosequencing analysis.

2.14 | Identification and quantification of colon short-chain fatty acids

Colon samples were suspended and homogenized in water. After centrifugation for 10 min at 12,000 rpm, the supernatant was collected and acidified by HCl. 4-Methylvaleric acid as internal standard was added into the supernatant at a final concentration of 258 μM. Short-chain fatty acids were identified and quantified by HP 5890 gas chromatograph configured with flame ionization detectors (Alrafas, Busbee, Nagarkatti, & Nagarkatti, 2019; Al-Ghezi, Miranda, et al., 2019). Data were collected using the Varian MS Workstation (version 6.9.2.) software. The linear regression equation was used to calculate the concentration of different short-chain fatty acids in colon samples.

2.15 | Effect of short-chain fatty acids on T cell functions

T cells were isolated from splenocytes by PE Selection Kit from STEMCELL Technologies (Cambridge, MA) according to the protocol from the company. The isolated T cells were cultured at 37°C in 5% CO_2 in the media supplemented with 10% FBS in the presence of 1-mM propionic acid (MilliporeSigma, St. Louis, MO) after stimulation with 1 $\mu g \cdot ml^{-1}$ of SEB. After culture for 3 days, the T cells were collected for proton efflux rate and culture supernatants were tested for cytokine quantification by ELISA.

2.16 | Measurement of proton efflux rate

Lung-associated mononuclear cells or purified T cells (2×10^5) were seeded in each well in XFp cell culture plate (Agilent, Santa Clara, CA) pre-coated with Cell-Tak (Corning, Corning, NY) to adhere seeded cells onto the bottom of wells during analysis. Glycolysis Rate Assay kit (Agilent) was used for the measurement of proton efflux rate in the lung-associated mononuclear cells and purified T cells according to the manufacturer's protocol. Briefly, Seahorse XF Base Medium without phenol red was enriched with 2-mM **glutamine**, 10-mM **pyruvate** and 5-mM HEPES, then the pH was adjusted at ~7.4. Injection cartridge (Agilent) was used to deliver different assay chemicals while performing GRA to achieve final concentrations of 5 μM of rotenone/antimycin A (Rot/AA) and 500-mM 2-deoxyglucose (2-DG) in each well. About every 3 min, the Seahorse XFp system measured the concentrations of oxygen and changes in pH values in the wells and converted them as oxygen consumption rate and extracellular acidification rate, respectively. Lastly, Desktop Report Generator software (Agilent) was used to interpret the acquired data and calculate proton efflux rate in the lung-associated mononuclear cells and purified T cells (Neamah et al., 2019).

2.17 | Data and analysis

The data and statistical analysis comply with the recommendations of the *British Journal of Pharmacology* on experimental design and analysis in pharmacology (Curtis et al., 2018). Power analysis was carried out (a = 0.05 and 1 − b = 0.80) to estimate the number of animals used in this study, which yielded a minimum sample size of five mice per group. Statistical analysis was undertaken only for studies where each group size was at least n = 5. All *in vitro* studies were carried out in triplicate. All *in vivo* studies were performed with at least five mice in each group. Statistical analysis was performed using the data generated for individual mice and not using replicates as independent values. All outliers were included in data analysis and presentation. GraphPad (RRID:SCR_002798) Prism 8.0 software was used in the statistical analysis. Student's unpaired t-test was used to compare two groups, whereas multiple comparisons were made using one-way ANOVA, followed by post hoc analysis using Tukey's method. The post hoc test was performed only if we noted an overall statistically significant difference in group means. For linear discriminant analysis (LDA) calculation, Galaxy (RRID:SCR_014609) online software (huttenhower.sph.harvard.edu/galaxy) was used to run LEfSe (RRID:SCR_014609) and create LDA and cladogram plots based on α value for the factorial Kruskal–Wallis test among classes, α value for the pairwise Wilcoxon test between subclasses and threshold on the logarithmic LDA score for discriminative features ≥2 unless stated differently. A P-value of <0.05 was considered statistically significant (Segata et al., 2011).

2.18 | Materials

Staphylococcus enterotoxin B (SEB) was purchased from Toxin Technologies (Sarasota, FL, USA). Delta-9-Tetrahydrocannabinol (THC) was procured from (NIH National Institute on Drug Abuse, National Institutes of Health, Bethesda, MD, USA). The following reagents (culture medium reagents: RPMI 1640, L-Glutamine, Penicillin-Streptomycin, HEPES, FBS, and PBS) were purchased from Invitrogen Life Technologies (Carlsbad, CA). We purchased the following antibodies and Fix/Perm buffer from Biolegend (San Diego, CA, USA). Fc Block reagent was purchased from BD Pharmingen (Carlsbad, CA). True-Nuclear™ Transcription Factor Buffer Set was purchased from BioLegend. RNeasy and miRNAeasy Mini kits, miScript primer assays kit, and miScript SYBR Green PCR kit were purchased from QIAGEN (QIAGEN, Valencia, CA). iScript and miScript cDNA synthesis kits were purchased from Bio-Rad (Madison, WI) and Epicentre's PCR premix F and Platinum Taq DNA Polymerase kits were purchased from Invitrogen Life Technologies (Carlsbad, CA). Ficoll-Histopaque®-1077

(Sigma-Aldrich) ELISA kits for (ELISA MAXTM Standard SET Mouse) were purchased from Biolegend. Immunofluorescence antibodies were purchased from Abcam (Cambridge, MA) PBS twice.

2.19 | Nomenclature of targets and ligands

Key protein targets and ligands in this article are hyperlinked to corresponding entries in the IUPHAR/BPS Guide to PHARMACOLOGY http://www.guidetopharmacology.org and are permanently archived in the Concise Guide to PHARMACOLOGY 2019/20 (Alexander et al., 2019).

3 | RESULTS

3.1 | Role of THC in the inhibition of ARDS

Our previous study demonstrated that treatment of mice with THC prior to SEB exposure attenuates lung injury through miRNA 17–92 cluster in ARDS mouse model (Rao et al., 2015). Because SEB is a superantigen that triggers acute inflammation, in the current study, we tested if treatment with THC after SEB sensitization would attenuate lung inflammation. Histopathological analysis demonstrated that THC could attenuate acute lung injury, reduce congestion and minimize fibrin in mice with ARDS, which was accompanied by a decrease in the infiltration of the immune cells in the lung tissues when compared to vehicle controls (Figure 1a). THC also significantly decreased the serum levels of pro-inflammatory cytokines including TNF-α, IFN-γ, CCL5 and MCP-1 but increased the serum levels of anti-inflammatory cytokines, such as TGF-β in ARDS mice when compared to vehicle control group (Figure 1b). THC significantly decreased the number of mononuclear cells isolated from the lungs from ARDS mice (Figure 1c). THC also significantly decreased the numbers of T cells, $CD4^+$ T cells and $CD8^+$ T cells in the lungs from ARDS mice (Figure 1d). In addition, THC significantly decreased the proton efflux rate in the mononuclear cells isolated from the lungs from ARDS mice, suggesting that THC may suppress glycolysis in cell metabolism (Figure 1e). These data together demonstrated that THC attenuates SEB-mediated inflammation in the lungs.

3.2 | Effects of THC on the regulation of microbial dysbiosis in ARDS

We were interested in the understanding of the functions of THC in the regulation of microbial dysbiosis in ARDS. Our pyrosequencing analysis demonstrated that THC dramatically altered microbiota in the lung tissues as shown in both the principal co-ordinator analysis (PCoA) β-diversity plot (revealing the clustering patterns) and cladogram (displaying potential microbial biomarkers) from linear discriminant analysis effect size (LEfSe) analysis (Figure 2a). THC also considerably changed microbiota in the colon (Figure 2b). The microbial species-level analysis in the lungs revealed that THC significantly increased the species of *Ruminococcus gnavus* but significantly decreased the species of *Bacteroides acidifaciens* and *Akkermansia muciniphila* in the lungs from ARDS mice (Figure 2c). Similarly, THC significantly increased the species of *R. gnavus* but significantly decreased the species of *A. muciniphila* in the colon from ARDS mice (Figure 3d). In addition, our analysis also showed that THC altered the microbiota in the blood from ARDS mice (Figure S1A). Similar to the lungs and colon, THC significantly increased the species of *R. gnavus* but significantly decreased the species of *A. muciniphila* in the blood from ARDS mice (Figures S1B and S2). The results demonstrated that THC could significantly increase the species of *R. gnavus* but significantly decrease the species of *A. muciniphila* systemically following SEB exposure.

R. gnavus could be considered as beneficial bacteria because it modulates mucin in the mucus which is a protective layer in many lining tissues in the body (Graziani et al., 2016). Thus, we examined mucin expression in the lung by immunofluorescence staining. We found that THC significantly inhibited the expression of mucin Muc5ac (Figure 2e) but significantly increased the expression mucin MUC5b (Figure 2f). It has been reported that MUC5ac is associated with inflammation and airway obstruction (Bonser & Erle, 2017), whereas Muc5b plays a role in mucociliary clearance, controlling infections in the airways and maintaining immune homeostasis in mouse lungs (Roy et al., 2014). Additionally, THC significantly inhibited Evans blue extravasation in the lungs and FITC-dextran levels in the serum, thereby suggesting that THC was blocking the vascular leak induced by SEB (Figure 2g). Similarly, THC significantly inhibited the concentrations of **LPS** in the bronchoalveolar lavage fluid and serum of SEB-exposed mice (Figure 2h).

3.3 | Effect of THC in the regulation of gene expression in lung epithelial cells

Because lung epithelial cells play a crucial role in barrier integrity and many other functions, we next examined the expression of genes in these cells from ARDS mice after THC treatment. To that end, we performed transcriptome array analysis using total RNAs isolated from the lung epithelial cells. Data obtained from the transcriptome array analysis showed altered expression of a large number of genes in the epithelial cells after THC treatment (Figure 3). Specifically, the scatter plot analysis demonstrated dysregulation of 1,553 genes in the epithelial cells from ARDS mice after THC treatment (Figure 3a). The 29 most significantly dysregulated genes induced by THC were shown in the heat map (Figure 3b). Among the 29 dysregulated genes, several genes were particularly related to antimicrobial enzymes, antimicrobial peptides, tight junction proteins and mucins (Figure 3b). The up-regulation of antimicrobial enzyme genes including Lyz1 and Lyz2 and antimicrobial peptide gene Defb2 and the down-regulation of antimicrobial peptide gene Defb1 were validated by real-time PCR (Figure 3c). Tight junction protein genes including **claudin**, Zo-1 and occludin-1 were up-regulated after THC treatment (Figure 3d). Mucin2 and Muc5b genes were also up-regulated significantly in the lung epithelial cells from ARDS mice after THC treatment (Figure 3e).

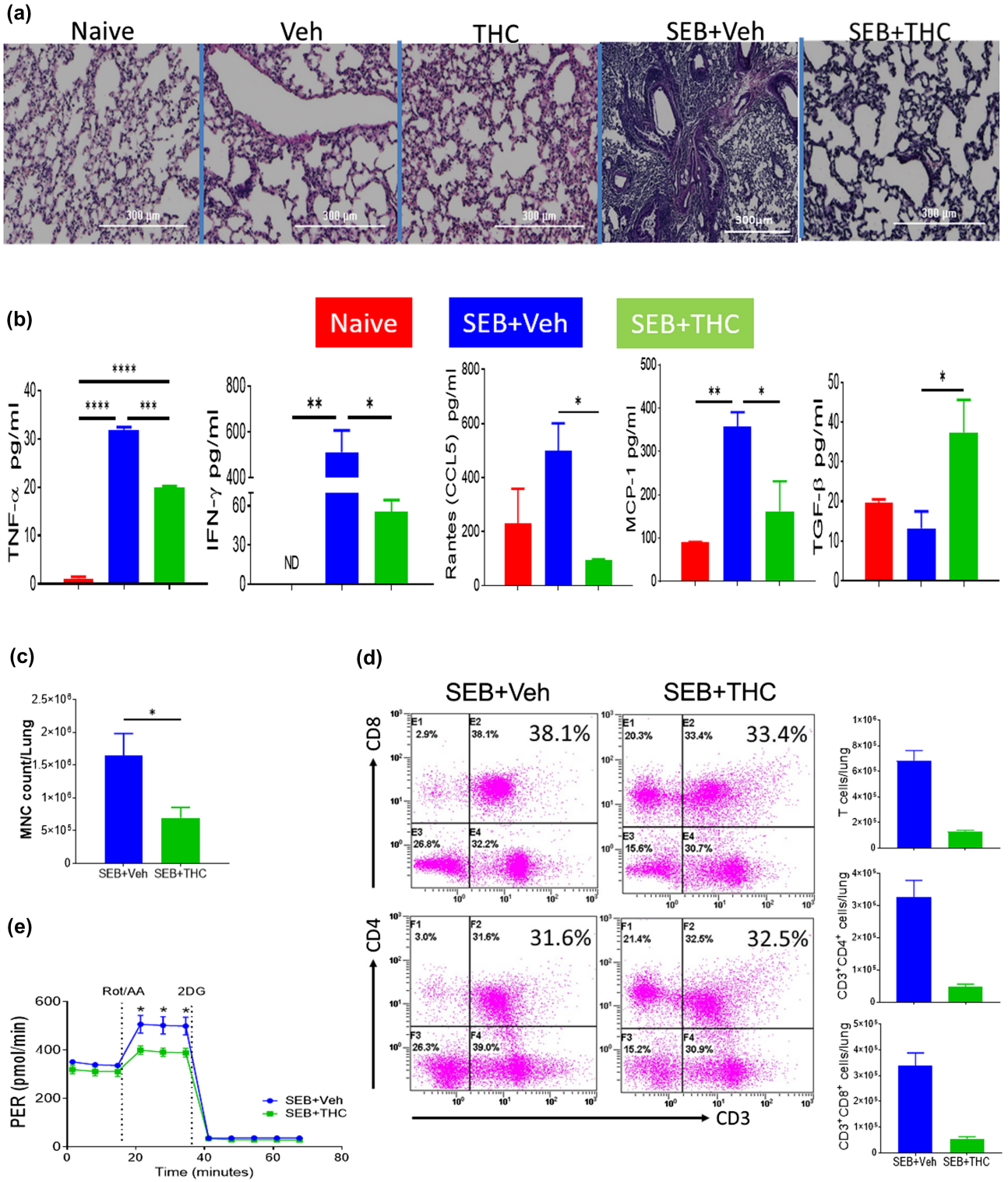

FIGURE 1 Effect of Δ^9-tetrahydrocannabinol (THC) on lung inflammation in staphylococcal enterotoxin-B (SEB)-induced acute respiratory distress syndrome (ARDS). C3H mice were injected with SEB followed by THC or vehicle as described in Section 2. Representative images of histopathological H&E staining sections of excised lung tissues in low power (4×) were shown (a). ELISA was used in the measurement of serum cytokines and chemokines (b). The change in total number of mononuclear cells isolated from the lungs was shown (c). Flow cytometry was used in the analysis of changes of $CD3^+$, $CD3^+CD4^+$ and $CD3^+CD8^+$ T cells in the lung-associated mononuclear cells from ARDS mice after THC treatment and a statistical bar graph is on the right of the flow (d). The inhibitory effect of THC on the proton efflux rate (PER) on $CD3^+$ T cells (e). Vertical bars represent data expressed as mean ± SEM with five mice in each group. *P*-value of <0.05 was considered statistically significant, $^*P < 0.05$

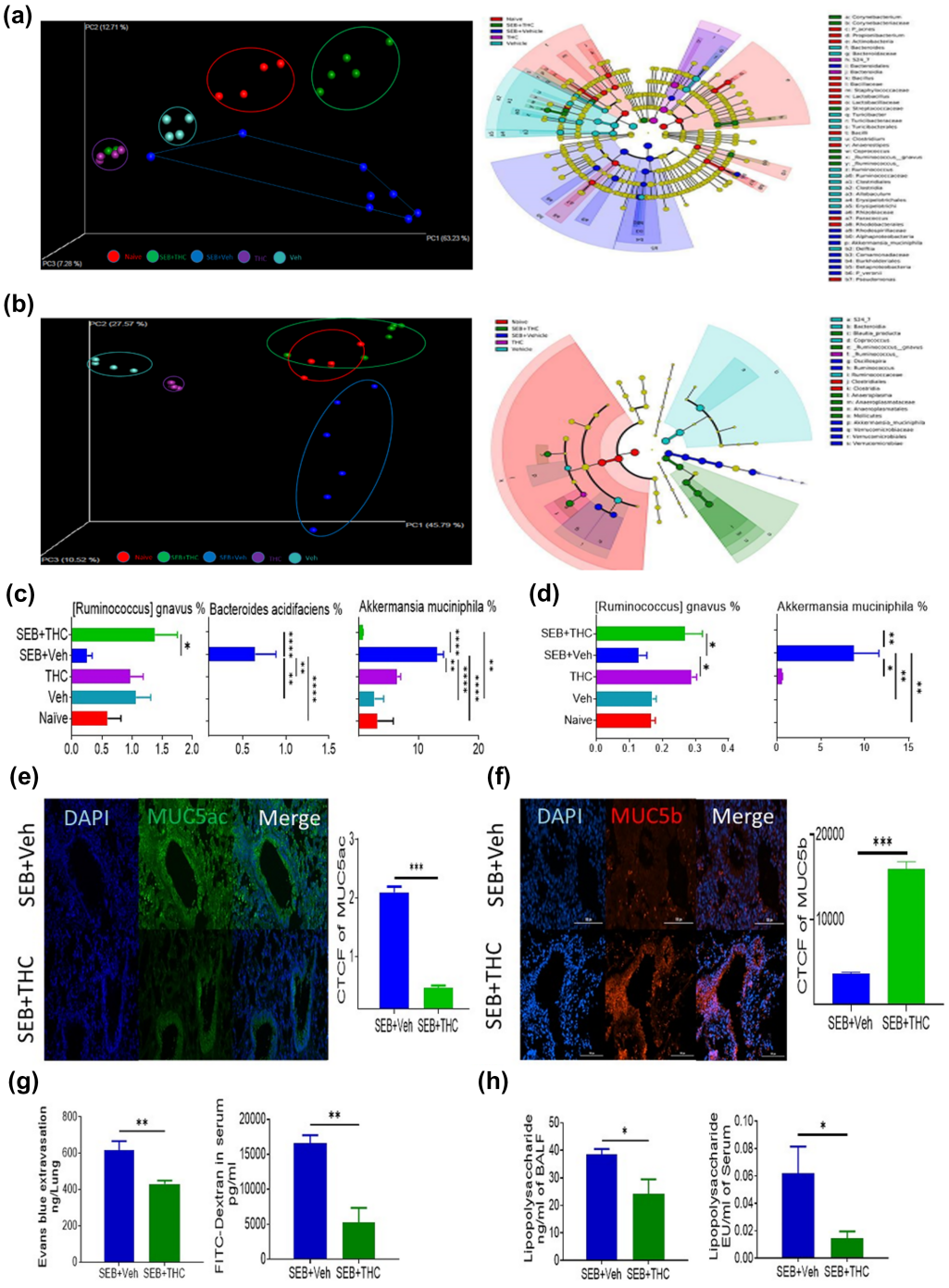

FIGURE 2 Effects of Δ^9-tetrahydrocannabinol (THC) on the abundance of microbiota in the lung and colon from acute respiratory distress syndrome (ARDS) mice. Lung and colon content samples were collected from different treatment groups described in Figure 1 and microbial communities compositions were determined by 16S rRNA sequencing and analysed by using quantitative insight into microbial ecology (QIIME) through Nephele platform. The effects of THC on microbiota compositions in the lung tissues were shown in the principal coordinator analysis β-diversity plot (revealing the clustering patterns) on the left and cladogram (displaying potential microbial biomarkers) from linear discriminant analysis effect size (LEfSe) analysis on the right (a). Similarly, the effects of THC on microbiota compositions in the colon were displayed in the principal coordinator analysis β-diversity plot on the left and cladogram from LEfSe analysis on the right (b). The effects of THC on the abundances of bacterial species including *Ruminococcus gnavus*, *Bacteroides acidifaciens* and *Akkermansia muciniphila* in the lung were depicted (c). The effects of THC on the abundances of bacterial species including *R. gnavus* and *A. muciniphila* in the colon were depicted (d). The effect of THC on the expression of MUC5ac in the lung tissues was determined by immunofluorescence staining and exhibited (e). The effect of THC on the expression of MUC5b in the lung tissues was determined by immunofluorescence staining and presented (f). The effect of THC on lung vascular permeability was determined by the measurement of concentrations of Evans blue in the lung tissues and FITC-dextran in the serum (g). The effects of THC on the concentrations of LPS in the bronchoalveolar lavage fluid (BALF) and serum were shown (h). Data were presented as mean ± SEM of multiple experiments from eight mice in each group. *P*-value of <0.05 was considered statistically significant, $^*P < 0.05$

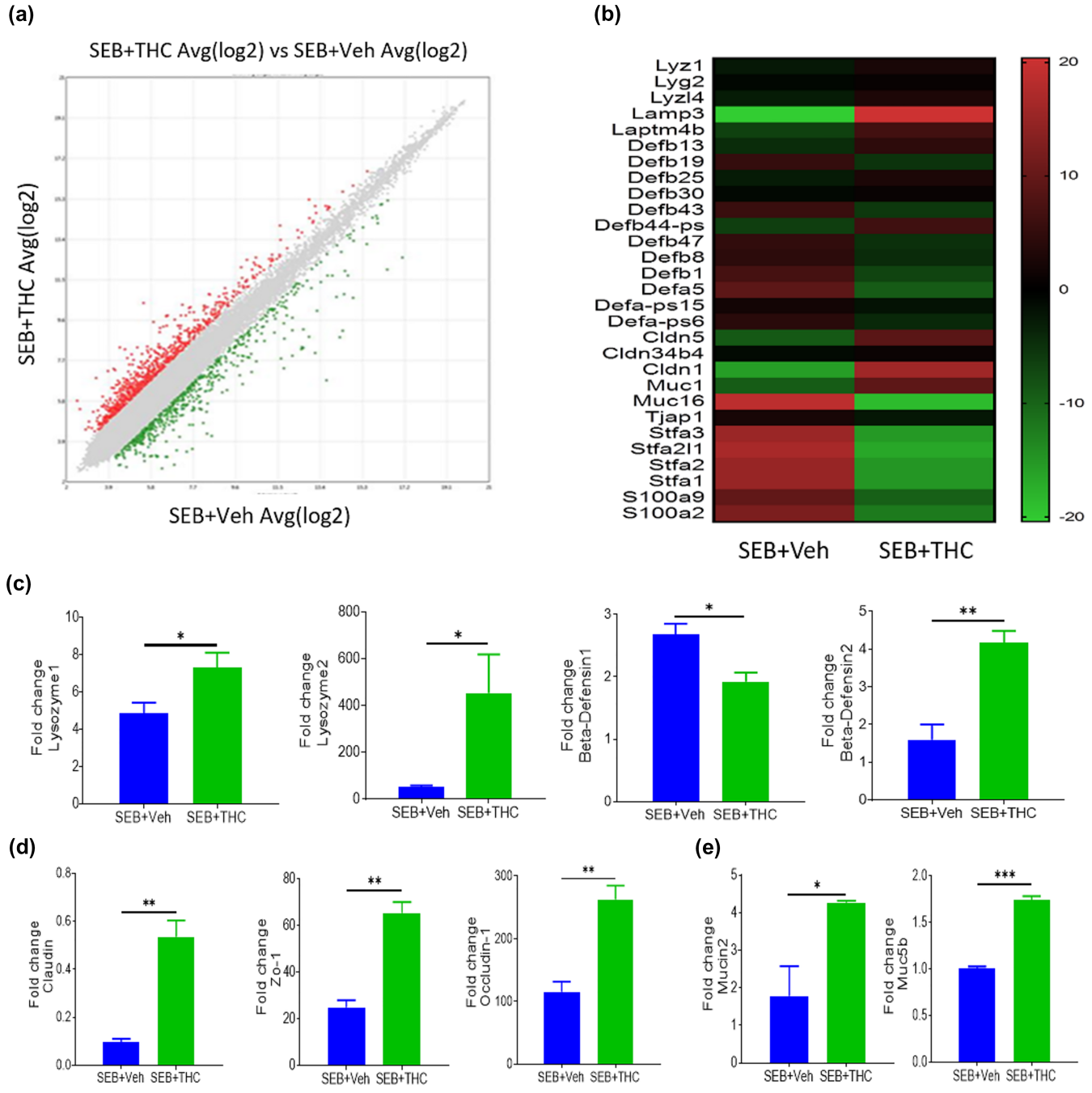

FIGURE 3 Effect of Δ^9-tetrahydrocannabinol (THC) on the transcriptional profiles of gene expression in the pulmonary epithelial cells from staphylococcal enterotoxin-B (SEB)-induced acute respiratory distress syndrome (ARDS). Lung epithelial cells were isolated from mice which were challenged with SEB followed by THC or vehicle as described in the Figure 1 legend. The differences of gene expression between THC-treated group and vehicle control group were shown in the scatter plot (a). The expression differences of selected genes between THC-treated group and vehicle control group were presented in the heat map (b). Quantitative validations of the differential expressions of genes have been presented, including lysozyme1, lysozyme2, β-defensin-1 and β-defensin-2 (c); claudin, Zo-1 and occludin-1 (d); and Mucin2 and Muc5b (e). Data were presented as mean ± SEM of multiple experiments from five mice in each group. *P*-value of <0.05 was considered statistically significant, $^*P < 0.05$

It has been reported that the epithelial tissue secretes different antimicrobial peptides to fight against different microorganisms (Gordon, Romanowski, & McDermott, 2005). These results suggested that THC may regulate the pathogenic microbiota promoted by SEB through induction of antimicrobial peptides.

3.4 | Effects of faecal microbiota transplantation on SEB-mediated ARDS

Faecal microbiota transplantation has been shown to replenish bacterial balance (Tauxe et al., 2015). Thus, faecal microbiota

transplantation was used to test the role of THC-induced microbial dysbiosis in the attenuation of ARDS. To that end, colonic material was obtained from different treatment groups including controls, THC, SEB + Veh and SEB + THC-treated groups and transplanted into recipient mice that had been treated with antibiotics for 4 weeks and then exposed to SEB. The fact that this antibiotic treatment was effective in depletion of microbes has been shown in Figure S3. Survival data showed that all SEB-challenged mice that received faecal microbiota transplantation from the SEB + Veh or vehicle alone group died within 10 days, whereas recipient mice that received faecal microbiota transplantation from the SEB + THC group showed 80% survival for more than 30 days (Figure 4a). Also, 60% of recipient mice that received faecal microbiota transplantation from the THC-alone-treated group survived SEB challenge. These data suggested that the microbiota from the SEB + THC group had protective effect on SEB-mediated pathogenesis. After faecal microbiota transplantation, colonic material was further examined for microbiota and we found that different treatment groups showed distinct clusters and composites of microbiota as shown in both the principal coordinator analysis β-diversity plot and cladogram from LEfSe analysis (Figure 4b,c). Linear discriminant analysis (LDA) showed that *R. gnavus* was seen only in the SEB + THC group and was increased by about three-fold compared to the SEB + Veh group (Figure 4d) consistent with the previous observation seen without faecal transfer (Figure 2c). We wish to clarify that Figure 4d shows LEfSe analysis based on the fold change (log differences) between the SEB + Veh and SEB + THC groups. In order to compare these two groups to find unique bacteria in each group, the results are depicted on the *X*-axis as LDA scores in opposite directions. This however does not mean that those depicted on the minus side are down-regulated. It shows that all those bacteria were uniquely expressed in that group and which were not expressed in the other group, with fold change. Thus, Proteobacteria phylum significantly decreased while Firmicutes phylum was significantly increased in mice that received faecal microbiota transplantation from the SEB + THC group when compared to mice that received faecal microbiota transplantation from the SEB + Veh group (Figure 4d,e).

Next, we tested if faecal microbiota transplantation could also induce alterations in immune cells in the lungs of recipient mice. After the faecal microbiota transplantation of colonic materials from SEB + THC-treated mice, the percentages of both $CD4^+$ and $CD8^+$ T cells significantly decreased in the lungs of recipient mice when compared with recipient mice that received faecal microbiota transplantation from the SEB + Veh-treated group (Figure 4f,g). In contrast, in the mice that received faecal microbiota transplantation from the SEB + THC-treated group, the percentages of immunosuppressive cells such as Tregs and MDSCs significantly increased in the lungs when compared to controls (Figure 4h,i). These data together suggested that THC-induced microbial dysbiosis was playing a beneficial role in suppressing SEB-induced ARDS pathogenesis.

3.5 | Effects of THC on short-chain fatty acids in ARDS

Because of the positive role played by THC-mediated microbial dysbiosis, we next measured short-chain fatty acids known to play anti-inflammatory role. Thus, we quantified the concentrations of short chain fatty acids in the colon flush from SEB + THC-treated mice and our data showed that the concentrations of propionic acid, butyric acid and acetic acid significantly increased in these mice when compared to the controls (Figure 5a). To further elucidate the role of short-chain fatty acids in inflammation, we used *in vitro* cultures of T cells activated with SEB in the presence of propionic acid. We found that in such cultures, addition of propionic acid significantly inhibited the production of pro-inflammatory cytokines including IFN-γ, IL-17 and IL-1β but significantly increased the production of anti-inflammatory cytokines such as IL-10 (Figure 5b). Flow cytometric analysis also showed that THC decreased the percentage and numbers of $CD3^+CD4^+$, $CD3^+CD8^+$, $NK1.1^+$ and IFN-γ^+ cells in these cultures (Figure S4). propionic acid also significantly inhibited the proton efflux rate in T cells after SEB activation (Figure 5c). These data suggested that SCFAs such as propionic acid suppressed the pro-inflammatory responses and thus may play a role in the control of ARDS pathogenesis.

4 | DISCUSSION

Acute respiratory distress syndrome (ARDS) is a life-threatening complication that can result following *Staphylococcus aureus* infection. The enterotoxin produced by these bacteria, staphylococcal enterotoxin-B (SEB), acts as a superantigen, thereby activating a large proportion of T cells expressing certain Vβ specificities leading to a cytokine storm and severe lung injury. Previous studies have shown that pro-inflammatory cytokines such as IL-1β, IL-6, IL-8 and TNF-α and inflammatory mononuclear cells are significantly increased in both ARDS patients and mice exposed to SEB (An et al., 2019; Badamjav et al., 2020; Johnson & Matthay, 2010; Mohammed et al., 2020). The current therapeutic approaches are inadequate because of which this devastating illness leads to high mortality rates, in the region of 30–40% (Zambon & Vincent, 2008). Because a significant proportion of COVID-19 patients develop ARDS, this incidence is further likely to increase. While microbiota found in the gut have been known to play a critical role in regulating inflammation, the role of resident microbiota during ARDS induced by SEB has not been investigated previously. In the current study, we make several important observations: (1) THC when administered after SEB exposure can attenuate SEB-mediated ARDS, (2) exposure to SEB induces dysbiosis in the lungs and gut, (3) THC triggers similar dysbiosis in the lungs and gut, and THC-mediated attenuation of ARDS depends on alterations in the microbiota and (4) faecal microbiota transplantation studies demonstrate that THC-mediated alterations in the lung microbiota may play a beneficial role in attenuating ARDS.

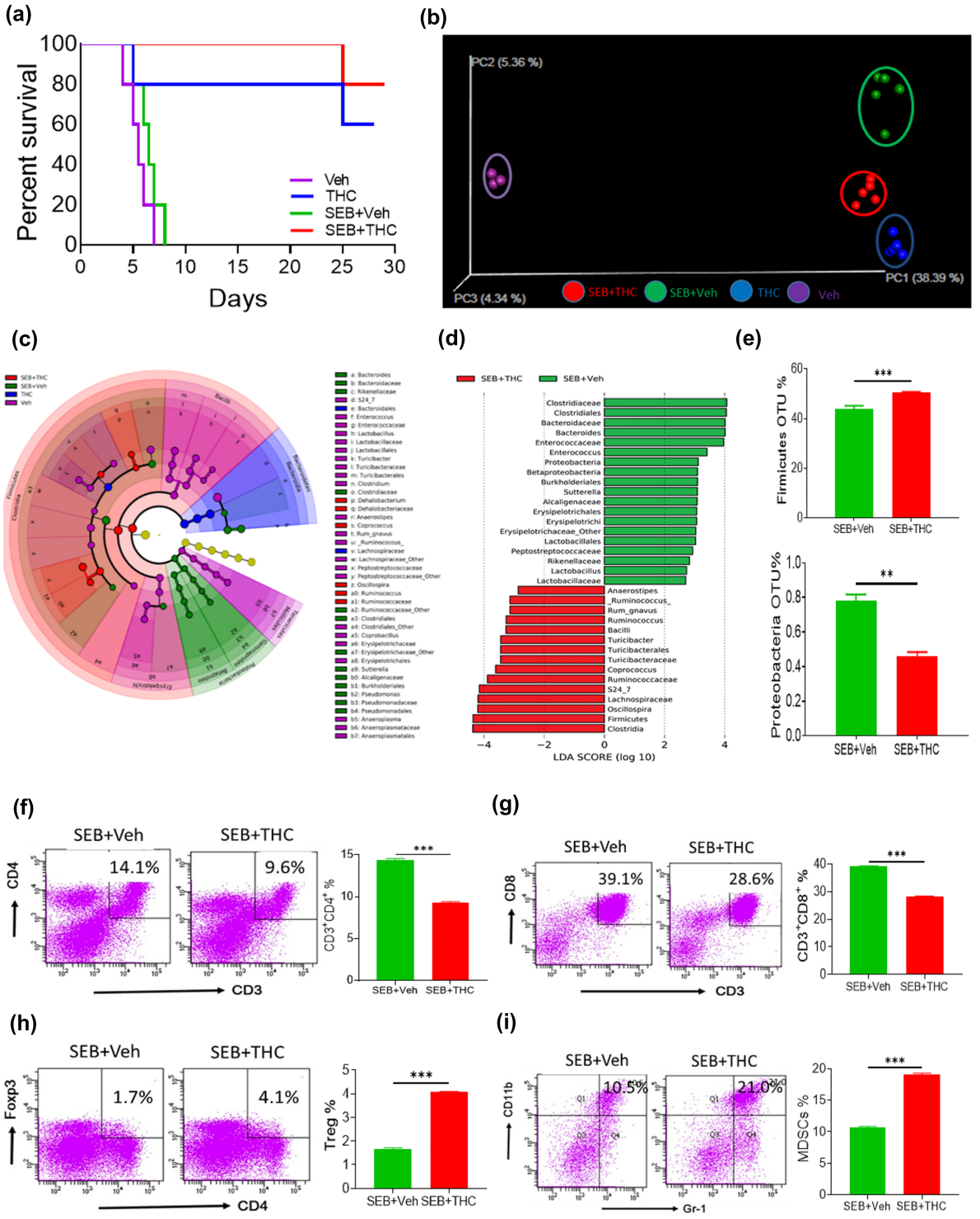

FIGURE 4 Effects of faecal microbiota transplantation (FMT) on microbiota reconstitution and acute respiratory distress syndrome (ARDS) pathogenesis. Colonic materials from various groups described in Figure 1 were transferred into antibiotic-microbiome-depleted recipient mice that were challenged with SEB. The survival of such recipient mice was studied (a). The effects of FMT of colonic materials from mice of different treatment groups on the microbiota reconstitution in the colon of ARDS recipient mice were displayed in the principal coordinator analysis (PCoA) β-diversity plot (b) and cladogram from LEfSe analysis (c). Linear discriminant analysis (LDA) scores were calculated for comparing differential abundance of microbiota in the colon from recipient mice after FMT of colonic materials from various groups and shown in the histogram plot (d). The effects of FMT of colonic materials from SEB + Veh and SEB + Δ^9-tetrahydrocannabinol (THC) groups on the bacterial abundances of Firmicutes and Proteobacteria phylum in the colon from ARDS recipient mice (e). The effects of FMT of colonic materials from SEB + Veh and SEB + THC groups on the percentages of $CD4^+$ T cells in the lungs (f), $CD8^+$ T cells (g), $CD4^+Foxp3^+$ Treg cells (h) and $CD11b^+Gr\text{-}1^+$ MDSCs (i). Vertical bars represent data expressed as mean ± SEM from groups of five mice. *P* value of <0.05 was considered statistically significant, $^*P < 0.05$

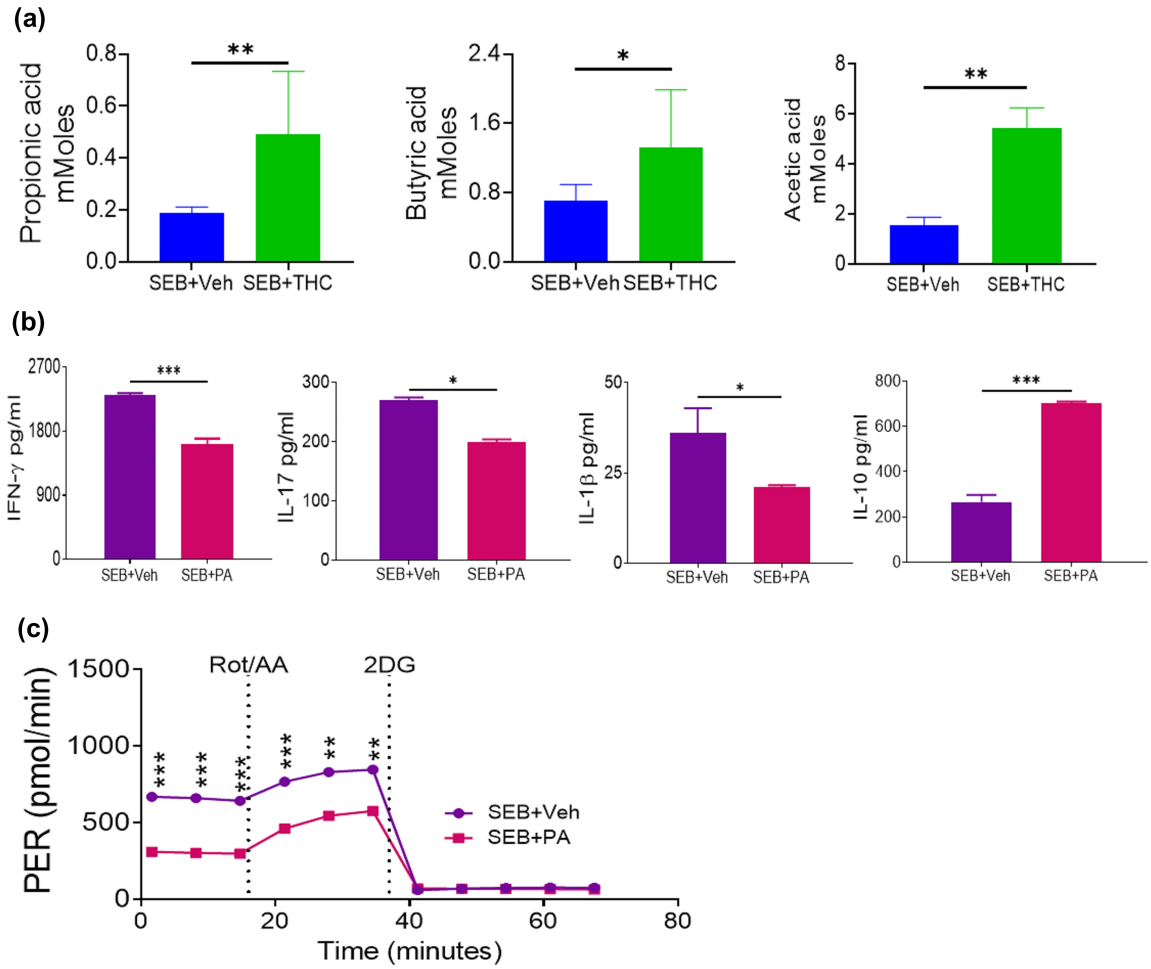

FIGURE 5 Effects of Δ^9-tetrahydrocannabinol (THC) on the production of short-chain fatty acids (SCFAs) and roles of propionic acid in T cells. Mice were treated with staphylococcal enterotoxin-B (SEB) followed by vehicle (SEB + Veh) or THC (SEB + THC) as described in Figure 1. Colon flush was collected and short-chain fatty acids quantified by HP 5890 gas chromatograph configured with flame ionization detectors. The effects of THC on the concentrations of propionic acid, butyric acid and acetic acid in the colon flush mice injected with SEB (a). Splenocytes harvested from naïve C3H/HeJ mice were cultured and activated with SEB along with propionic acid (PA). The effects of propionic acid on the production of IFN-γ, IL-17, IL-1β and IL-10 from in vitro cultured T cells after SEB activation was determined by ELISA (b). The effects of propionic acid on the proton efflux rate in cultured T cells after SEB activation was determined by a Seahorse XF24 analyser (c). Data were presented as mean ± SEM from five mice or five replicates in each group. *P*-value of <0.05 was considered statistically significant, $^*P < 0.05$,

Studies from our laboratory and elsewhere have shown that THC acts as a potent anti-inflammatory agent (Nagarkatti et al., 2009). For instance, THC could significantly decrease the levels of pro-inflammatory cytokines such as IFN-γ and TNF-α but increase anti-inflammatory cytokines such as IL-10 and TGF-β (Hernandez-Cervantes, Mendez-Diaz, Prospero-Garcia, & Morales-Montor, 2017; Zgair et al., 2017). Furthermore, THC has been shown to decrease Th1 cells while promoting Tregs and MDSCs (Eisenstein & Meissler, 2015; Hegde et al., 2010; Mohammed et al., 2020; Nagarkatti et al., 2009). These studies are consistent with our current findings that THC significantly inhibited infiltration of mononuclear cells in the lung, decreased serum levels of pro-inflammatory cytokines including TNF-α, IFN-γ, CCL5 and MCP-1, while increasing anti-inflammatory cytokines, TGF-β, decreased the number of CD3, $CD4^+$ and $CD8^+$ T cells and suppressed the proton efflux rate in the lung-associated mononuclear cells (Figure 1). Inflammation in the lung also triggers structural remodelling of the airway involving epithelial cells, including increased extracellular deposition and expansion of pro-fibrotic myofibroblast populations (Brasier, 2018).

A few recent studies revealed that THC could alter gut microbiota in diet-induced obesity and experimental autoimmune encephalomyelitis-induced mice (Al-Ghezi, Busbee, et al., 2019; Cluny, Keenan, Reimer, Le Foll, & Sharkey, 2015; Crost et al., 2013). Thus far, there are no studies delineating the effect of SEB or THC on lung microbiota. Thus, it was interesting to note that THC treatment in SEB-challenged mice led to similar changes in microbiota in both the gut and lungs inasmuch as we noted that THC significantly increased the abundance of bacterial species *R. gnavus* in Firmicutes phylum but decreased that of *A. muciniphila* (Figures 2 and S1). *R. gnavus* is a human gut symbiont and is known to play an important role in the regulation of mucin expression and glycosylation (Graziani et al., 2016). Specifically, *R. gnavus* increased the expression of

glycoproteins and Muc2 in goblet cells in the colonic mucosa from mice (Graziani et al., 2016). Mucin is one of the most important components of mucus and plays a crucial role in the defence against bacterial pneumonia, maintenance of the integrity of lung tissue and prevention of vascular leak (Johansson et al., 2011; Roy et al., 2014). Besides, *R. gnavus* produced peptides such as ruminococcin A (RumA) and RumC, have high activity against pathogenic clostridia and exhibit other antimicrobial activities (Balty et al., 2019; Ongey et al., 2018). In contrast, *A. muciniphila* is widely present in the intestines of humans and animals and known to induce IgG1 antibodies and antigen-specific T cell responses, thus enhancing immune responses (Ansaldo et al., 2019). Indeed, it has been reported that *A. muciniphila* increased the expression of pro-inflammatory cytokines such as IFN-γ, IP-10, TNF-α, IL-6, IL-12 and IL-17 in the colon and colonic tissues from mice (Ganesh, Klopfleisch, Loh, & Blaut, 2013). In addition, *A. muciniphila* has a specialized ability in mucin degradation and excessive mucin degradation may induce inflammation (Derrien, Belzer, & de Vos, 2017; Ganesh et al., 2013). These results suggested that THC could modulate microbial dysbiosis in the lung, particularly increase the abundance of *R. gnavus*, but decrease that of *A. muciniphila*, which were responsible for the induction of mucin expression, inhibition of the pro-inflammatory responses and suppression of pathogenic bacteria, leading to the attenuation of ARDS.

As epithelial cells play several important functions such as barrier protection, fluid balance, mucus and surfactant production and repair following injury, in the current study we investigated the effect of SEB and treatment with THC, on gene expression in lung epithelial cells. Our analysis showed that THC caused altered expression of over 1,553 genes in the lung epithelial cells from ARDS mice and, particularly, several dysregulated genes were related to antimicrobial enzymes, antimicrobial peptides, tight junction proteins and mucins (Figure 3a,b). Further study revealed that THC up-regulated the gene expression of mucins such as Mucin2 and Muc5b (Figure 3e) and tight junction proteins such as claudin, ZO-1 and occludin-1 in the lung epithelial cells from ARDS mice (Figure 3d). Mucins are highly glycosylated proteins, which are the major components of the mucous on the surface of respiratory and digestive tracts and protect epithelial cells from infection, dehydration and physical or chemical injury (Dhanisha, Guruvayoorappan, Drishya, & Abeesh, 2018; Ma, Rubin, & Voynow, 2018). THC treatment increased the production of tight junction proteins indicating its role in protecting cell integrity (Alhamoruni, Lee, Wright, Larvin, & O'Sullivan, 2010; Gigli et al., 2017). Therefore, THC may increase the gene expression of mucins and tight junction proteins and thus has protective effect during SEB-mediated ARDS. Most interestingly, our study discovered that THC up-regulated gene expression involving antimicrobial enzymes such as Lyz1 and Lyz2 and antimicrobial peptide gene Defb2, but down-regulated gene expression of other antimicrobial peptides such as Defb1, in the lung epithelial cells from ARDS mice (Figure 3). It has been reported that the host-derived antimicrobial enzymes such as lysozyme in the mucus protect from harmful bacteria (Oliver & Wells, 2015). There are other reports which have shown that lung injury is associated with alterations in β-defensins. For example, elevated β-defensin-1 protein was seen in chronic obstructive pulmonary disease (COPD) and severe asthma (Baines et al., 2015; Levy et al., 2005). Additionally, **β-defensin 2 (beta-defensin 4)** has been shown to play both an anti-inflammatory and antimicrobial role. Overexpression of β-defensin 2 was shown to protect against *Pseudomonas aeruginosa* and caecal ligation and double puncture-induced lung injury (Shu et al., 2006). Thus, the ability of SEB to induce β-defensin 2 and decrease β-defensin 1 correlates with the ARDS pathogenesis and in this context, it is interesting to note that THC reversed these effects.

While we did see significant dysbiosis following THC treatment, it was not clear if this played any role in the attenuation of SEB-mediated ARDS. To that end, we pursued faecal microbiota transplantation studies which conclusively demonstrated that THC-mediated alterations in microbiota play a crucial role in the attenuation of SEB-meditated ARDS. The most exciting finding was that antibiotic-treated mice that received faecal microbiota transplantation from the SEB + Veh group all died within 8 days of SEB challenge while those that received faecal microbiota transplantation from the SEB + THC group, 80%, survived beyond 30 days, thereby demonstrating that THC-mediated dysbiosis was playing a crucial role in attenuating SEB-induced ARDS. The fact that faecal microbiota transplantation from THC-alone-treated mice also provided 60% protection against SEB also supported the above findings. Thus, it is likely that THC-mediated increase in the abundance of beneficial bacteria such as *Ruminococcus* spp. in Firmicutes phylum and decrease in pathogenic bacteria in Proteobacteria phylum, may help in attenuating ARDS.

Recent studies have shown that short-chain fatty acids including acetate, propionate and butyrate are main bacterial metabolites and play critical roles in human health and diseases (Rios-Covian et al., 2016; Vinolo, Rodrigues, Nachbar, & Curi, 2011). Because THC could induce microbial dysbiosis in ARDS mice (Figures 3 and 4), it was expected that THC also affected the production of short-chain fatty acids. Our analysis showed that THC significantly increased the levels of propionic acid, butyric acid and acetic acid in the colon flash from ARDS mice (Figure 5). Furthermore, propionic acid significantly inhibited the production of pro-inflammatory cytokines but significantly increased the production of anti-inflammatory cytokines (Figure 5). It has been reported that short-chain fatty acids could activate G-coupled receptors, suppress histone deacetylases, affect energy metabolism and thus regulate inflammatory responses (Koh, De Vadder, Kovatcheva-Datchary, & Backhed, 2016). Specifically, short-chain fatty acids could inhibit the production of pro-inflammatory cytokines and suppress proliferation, activation and migration of immune cells (Vinolo et al., 2011). Investigations also discovered that *R. gnavus* produced propionate and propanol as the end products of metabolism (Crost et al., 2013). These results suggested that THC may increase the abundance of bacterial species such as *R. gnavus* in Firmicutes phylum, promote the production of short-chain fatty acids such as propionic acid and thus suppress the pro-inflammatory responses, resulting in the attenuation of acute lung injury. Thus, the faecal

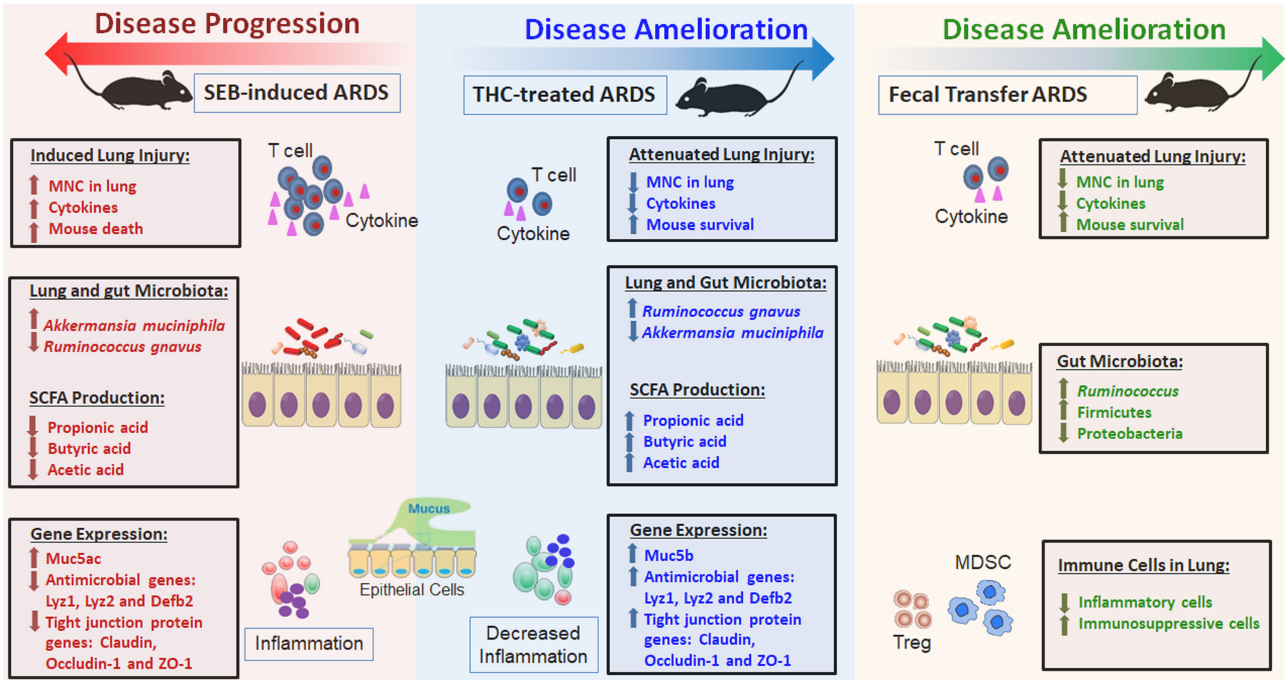

FIGURE 6 Schematic representation on how Δ^9-tetrahydrocannabinol (THC) and microbiota from THC-treated mice may attenuate staphylococcal enterotoxin-B (SEB)-mediated acute respiratory distress syndrome (ARDS) and mortality. SEB acts as a superantigen and triggers robust inflammation in the lungs leading to ARDS and death. SEB also causes dysbiosis in the lungs and gut with emergence of pathogenic bacteria. This is also accompanied by decrease in SCFA, increased expression of Muc5ac and decrease in antimicrobial peptides and tight junction proteins. This may lead to increased penetrance of pathogenic bacteria in the lungs and further aggravation of inflammation. Treatment with THC (SEB + THC group) leads to reversal of dysbiosis and other deleterious changes induced by SEB leading to survival of mice. Faecal microbiota transplantation (FMT) experiments demonstrate such that transfer of microbiota from THC-treated mice can also cause beneficial bacteria to colonize and suppress SEB-mediated ARDS, inflammation and mortality by also inducing an anti-inflammatory state consisting of regulatory T cells (Tregs) and myeloid-derived suppresser cells (MDSCs)

microbiota transplantation may have worked to attenuate ARDS because of the induction of SCFA.

In summary, the major findings in the current study have been summarized in Figure 6. This study demonstrates that SEB triggers ARDS which is accompanied by lung inflammation and similar dysbiosis in the lungs and gut. This is also accompanied by decrease in short-chain fatty acid, increased expression of Muc5ac and decrease in antimicrobial peptides and tight junction proteins. This may cause increased penetrance of pathogenic bacteria and enhanced lung inflammation and mortality. Treatment with THC (SEB + THC group) leads to reversal of dysbiosis and other deleterious changes induced by SEB leading to survival of mice. faecal microbiota transplantation experiments confirm that the effect of THC is mediated through alterations in microbiota because antibiotic-treated mice receiving faecal microbiota transplantation survive SEB challenge and exhibit decreased inflammation in the lungs which is associated with induction of Tregs and MDSCs and SCFA, which was shown in vitro to induce anti-inflammatory phenotype. Additionally, because a significant proportion of COVID-19 patients develop ARDS and cytokine storm, our studies raise a question on whether targeting cannabinoid receptors constitutes a therapeutic modality to treat ARDS in such patients.

ACKNOWLEDGEMENTS

The studies were supported in part by NIH grants: P01AT003961, P20GM103641, R01AT006888, R01ES030144, R01AI123947 and R01AI129788 awarded to M.N. and P.N. The Ministry of Higher Education and Scientific Research (MOHESR), Iraq, provided support to A.M. The funding agencies had no role in the experimental design, data collection and analysis, decision to publish, or preparation of the manuscript.

AUTHOR CONTRIBUTIONS

A.M., P.N. and M.N. designed all the experiments. A.M. performed all experiments under supervision of P.N. and M.N. A.M. collected and analysed data and wrote the manuscript. A.M. and H.A. contributed to microbiome metagenomic analysis. J.Z. revised first copy of the manuscript and which was approved by all authors. P.N. and M.N. supervised the work from designing to finalizing the manuscript for journal submission.

CONFLICT OF INTEREST

The authors declare no conflicts of interest and that there are no competing financial interests or personal relationship that could influence the work reported in this paper.

DECLARATION OF TRANSPARENCY AND SCIENTIFIC RIGOUR

This Declaration acknowledges that this paper adheres to the principles for transparent reporting and scientific rigour of preclinical research as stated in the *BJP* guidelines for Design & Analysis, Immunoblotting and Immunochemistry and Animal Experimentation, and as recommended by funding agencies, publishers and other organizations engaged with supporting research.

ORCID

Amira Mohammed https://orcid.org/0000-0001-8931-2219
Hasan K. Alghetaa https://orcid.org/0000-0001-6435-9328
Prakash Nagarkatti https://orcid.org/0000-0003-2663-0759
Mitzi Nagarkatti https://orcid.org/0000-0002-5977-5615

REFERENCES

Alexander, S. P., Fabbro, D., Kelly, E., Mathie, A., Peters, J. A., Veale, E. L., … Sharman, J. L. (2019). The Concise Guide to PHARMACOLOGY 2019/20: Enzymes. *British Journal of Pharmacology*, *176*(Suppl 1), S297–S396. https://doi.org/10.1111/bph.14752

Alghetaa, H., Mohammed, A., Sultan, M., Busbee, P., Murphy, A., Chatterjee, S., … Nagarkatti, P. (2018). Resveratrol protects mice against SEB-induced acute lung injury and mortality by miR-193a modulation that targets TGF-β signalling. *Journal of Cellular and Molecular Medicine*, *22*(5), 2644–2655. https://doi.org/10.1111/jcmm.13542

Al-Ghezi, Z. Z., Busbee, P. B., Alghetaa, H., Nagarkatti, P. S., & Nagarkatti, M. (2019). Combination of cannabinoids, delta-9-tetrahydrocannabinol (THC) and cannabidiol (CBD), mitigates experimental autoimmune encephalomyelitis (EAE) by altering the gut microbiome. *Brain, Behavior, and Immunity*, *82*, 25–35. https://doi.org/10.1016/j.bbi.2019.07.028

Al-Ghezi, Z. Z., Miranda, K., Nagarkatti, M., & Nagarkatti, P. S. (2019). Combination of cannabinoids, Δ9-tetrahydrocannabinol and cannabidiol, ameliorates experimental multiple sclerosis by suppressing neuroinflammation through regulation of miRNA-mediated signaling pathways. *Frontiers in Immunology*, *10*, 1921. https://doi.org/10.3389/fimmu.2019.01921

Alhamoruni, A., Lee, A. C., Wright, K. L., Larvin, M., & O'Sullivan, S. E. (2010). Pharmacological effects of cannabinoids on the Caco-2 cell culture model of intestinal permeability. *The Journal of Pharmacology and Experimental Therapeutics*, *335*(1), 92–102. https://doi.org/10.1124/jpet.110.168237

Alharris, E., Alghetaa, H., Seth, R., Chatterjee, S., Singh, N. P., Nagarkatti, M., & Nagarkatti, P. (2018). Resveratrol attenuates allergic asthma and associated inflammation in the lungs through regulation of miRNA-34a that targets FoxP3 in mice. *Frontiers in Immunology*, *9*, 2992. https://doi.org/10.3389/fimmu.2018.02992

Alrafas, H. R., Busbee, P. B., Nagarkatti, M., & Nagarkatti, P. S. (2019). Resveratrol modulates the gut microbiota to prevent murine colitis development through induction of Tregs and suppression of Th17 cells. *Journal of Leukocyte Biology*, *106*(2), 467–480. https://doi.org/10.1002/JLB.3A1218-476RR

An, X., Sun, X., Hou, Y., Yang, X., Chen, H., Zhang, P., & Wu, J. (2019). Protective effect of oxytocin on LPS-induced acute lung injury in mice. *Scientific Reports*, *9*(1), 2836. https://doi.org/10.1038/s41598-019-39349-1

Ansaldo, E., Slayden, L. C., Ching, K. L., Koch, M. A., Wolf, N. K., Plichta, D. R., … Barton, G. M. (2019). *Akkermansia muciniphila* induces intestinal adaptive immune responses during homeostasis. *Science*, *364*(6446), 1179–1184. https://doi.org/10.1126/science.aaw7479

Badamjav, R., Sonom, D., Wu, Y., Zhang, Y., Kou, J., Yu, B., & Li, F. (2020). The protective effects of *Thalictrum minus* L. on lipopolysaccharide-induced acute lung injury. *Journal of Ethnopharmacology*, *248*, 112355. https://doi.org/10.1016/j.jep.2019.112355

Baines, K. J., Wright, T. K., Simpson, J. L., McDonald, V. M., Wood, L. G., Parsons, K. S., … Gibson, P. G. (2015). Airway β-defensin-1 protein is elevated in COPD and severe asthma. *Mediators of Inflammation*, *2015*, 407271–407278. https://doi.org/10.1155/2015/407271

Balty, C., Guillot, A., Fradale, L., Brewee, C., Boulay, M., Kubiak, X., … Berteau, O. (2019). Ruminococcin C, an anti-clostridial sactipeptide produced by a prominent member of the human microbiota *Ruminococcus gnavus*. *The Journal of Biological Chemistry*, *294*(40), 14512–14525. https://doi.org/10.1074/jbc.RA119.009416

Bonser, L. R., & Erle, D. J. (2017). Airway mucus and asthma: The role of MUC5AC and MUC5B. *Journal of Clinical Medicine*, *6*(12). https://doi.org/10.3390/jcm6120112

Borner, C., Smida, M., Hollt, V., Schraven, B., & Kraus, J. (2009). Cannabinoid receptor type 1- and 2-mediated increase in cyclic AMP inhibits T cell receptor-triggered signaling. *The Journal of Biological Chemistry*, *284*(51), 35450–35460. https://doi.org/10.1074/jbc.M109.006338

Brasier, A. R. (2018). Therapeutic targets for inflammation-mediated airway remodeling in chronic lung disease. *Expert Review of Respiratory Medicine*, *12*(11), 931–939. https://doi.org/10.1080/17476348.2018.1526677

Chapman, H. A., Li, X., Alexander, J. P., Brumwell, A., Lorizio, W., Tan, K., … Vu, T. H. (2011). Integrin α6β4 identifies an adult distal lung epithelial population with regenerative potential in mice. *The Journal of Clinical Investigation*, *121*(7), 2855–2862. https://doi.org/10.1172/JCI57673

Chevalier, C., Stojanović, O., Colin, D. J., Suarez-Zamorano, N., Tarallo, V., Veyrat-Durebex, C., … Montet, X. (2015). Gut microbiota orchestrates energy homeostasis during cold. *Cell*, *163*(6), 1360–1374. https://doi.org/10.1016/j.cell.2015.11.004

Cluny, N. L., Keenan, C. M., Reimer, R. A., Le Foll, B., & Sharkey, K. A. (2015). Prevention of diet-induced obesity effects on body weight and gut microbiota in mice treated chronically with Δ^9-tetrahydrocannabinol. *PLoS ONE*, *10*(12), e0144270. https://doi.org/10.1371/journal.pone.0144270

Cox, M. J., Turek, E. M., Hennessy, C., Mirza, G. K., James, P. L., Coleman, M., … Loebinger, M. R. (2017). Longitudinal assessment of sputum microbiome by sequencing of the 16*S* rRNA gene in non-cystic fibrosis bronchiectasis patients. *PLoS ONE*, *12*(2), e0170622. https://doi.org/10.1371/journal.pone.0170622

Crost, E. H., Tailford, L. E., Le Gall, G., Fons, M., Henrissat, B., & Juge, N. (2013). Utilisation of mucin glycans by the human gut symbiont *Ruminococcus gnavus* is strain-dependent. *PLoS ONE*, *8*(10), e76341. https://doi.org/10.1371/journal.pone.0076341

Curtis, M. J., Alexander, S., Cirino, G., Docherty, J. R., George, C. H., Giembycz, M. A., … Ahluwalia, A. (2018). Experimental design and analysis and their reporting II: Updated and simplified guidance for authors and peer reviewers. *British Journal of Pharmacology*, *175*(7), 987–993. https://doi.org/10.1111/bph.14153

Das, B., & Nair, G. B. (2019). Homeostasis and dysbiosis of the gut microbiome in health and disease. *J Biosci*, *44*(5). Retrieved from https://www.ncbi.nlm.nih.gov/pubmed/31719226

Derrien, M., Belzer, C., & de Vos, W. M. (2017). *Akkermansia muciniphila* and its role in regulating host functions. *Microbial Pathogenesis*, *106*, 171–181. https://doi.org/10.1016/j.micpath.2016.02.005

Dhanisha, S. S., Guruvayoorappan, C., Drishya, S., & Abeesh, P. (2018). Mucins: Structural diversity, biosynthesis, its role in pathogenesis and as possible therapeutic targets. *Critical Reviews in Oncology/Hematology*, *122*, 98–122. https://doi.org/10.1016/j.critrevonc.2017.12.006

Dopkins, N., Nagarkatti, P. S., & Nagarkatti, M. (2018). The role of gut microbiome and associated metabolome in the regulation of neuroinflammation in multiple sclerosis and its implications in attenuating

chronic inflammation in other inflammatory and autoimmune disorders. *Immunology*, *154*(2), 178–185. https://doi.org/10.1111/imm.12903

Eisenstein, T. K., & Meissler, J. J. (2015). Effects of cannabinoids on T-cell function and resistance to infection. *Journal of Neuroimmune Pharmacology*, *10*(2), 204–216. https://doi.org/10.1007/s11481-015-9603-3

Elliott, D. M., Nagarkatti, M., & Nagarkatti, P. S. (2016). 3,3′-Diindolylmethane ameliorates staphylococcal enterotoxin B-induced acute lung injury through alterations in the expression of microRNA that target apoptosis and cell-cycle arrest in activated T cells. *The Journal of Pharmacology and Experimental Therapeutics*, *357*(1), 177–187. https://doi.org/10.1124/jpet.115.226563

Ganesh B. P., Klopfleisch R., Loh G., & Blaut M. (2013). Commensal Akkermansia muciniphila Exacerbates Gut Inflammation in Salmonella Typhimurium-Infected Gnotobiotic Mice. *PLoS ONE*, *8*(9), e74963. https://doi.org/10.1371/journal.pone.0074963

Gigli, S., Seguella, L., Pesce, M., Bruzzese, E., D'Alessandro, A., Cuomo, R., … Esposito, G. (2017). Cannabidiol restores intestinal barrier dysfunction and inhibits the apoptotic process induced by *Clostridium difficile* toxin A in Caco-2 cells. *United European Gastroenterology Journal*, *5*(8), 1108–1115. https://doi.org/10.1177/2050640617698622

Gordon Y. J., Romanowski E. G., & McDermott A. M. (2005). A Review of Antimicrobial Peptides and Their Therapeutic Potential as Anti-Infective Drugs. *Current Eye Research*, *30*(7), 505–515. https://doi.org/10.1080/02713680590968637

Graziani, F., Pujol, A., Nicoletti, C., Dou, S., Maresca, M., Giardina, T., … Perrier, J. (2016). *Ruminococcus gnavus* E1 modulates mucin expression and intestinal glycosylation. *Journal of Applied Microbiology*, *120*(5), 1403–1417. https://doi.org/10.1111/jam.13095

Grivennikov, S. I., Wang, K., Mucida, D., Stewart, C. A., Schnabl, B., Jauch, D., … Karin, M. (2012). Adenoma-linked barrier defects and microbial products drive IL-23/IL-17-mediated tumour growth. *Nature*, *491*(7423), 254–258. https://doi.org/10.1038/nature11465

Hegde, V. L., Nagarkatti, M., & Nagarkatti, P. S. (2010). Cannabinoid receptor activation leads to massive mobilization of myeloid-derived suppressor cells with potent immunosuppressive properties. *European Journal of Immunology*, *40*(12), 3358–3371. https://doi.org/10.1002/eji.201040667

Henry, B. M., & Lippi, G. (2020). Poor survival with extracorporeal membrane oxygenation in acute respiratory distress syndrome (ARDS) due to coronavirus disease 2019 (COVID-19): Pooled analysis of early reports. *Journal of Critical Care*, *58*, 27–28. https://doi.org/10.1016/j.jcrc.2020.03.011

Hernandez-Cervantes, R., Mendez-Diaz, M., Prospero-Garcia, O., & Morales-Montor, J. (2017). Immunoregulatory role of cannabinoids during infectious disease. *Neuroimmunomodulation*, *24*(4–5), 183–199. https://doi.org/10.1159/000481824

Huzella, L. M., Buckley, M. J., Alves, D. A., Stiles, B. G., & Krakauer, T. (2009). Central roles for IL-2 and MCP-1 following intranasal exposure to SEB: A new mouse model. *Research in Veterinary Science*, *86*(2), 241–247. https://doi.org/10.1016/j.rvsc.2008.07.020

Johansson, M. E., Ambort, D., Pelaseyed, T., Schütte, A., Gustafsson, J. K., Ermund, A., … van der Post, S. (2011). Composition and functional role of the mucus layers in the intestine. *Cellular and Molecular Life Sciences*, *68*(22), 3635–3641. https://doi.org/10.1007/s00018-011-0822-3

Johnson, E. R., & Matthay, M. A. (2010). Acute lung injury: Epidemiology, pathogenesis, and treatment. *Journal of Aerosol Medicine and Pulmonary Drug Delivery*, *23*(4), 243–252. https://doi.org/10.1089/jamp.2009.0775

Koh, A., De Vadder, F., Kovatcheva-Datchary, P., & Backhed, F. (2016). From dietary fiber to host physiology: Short-chain fatty acids as key bacterial metabolites. *Cell*, *165*(6), 1332–1345. https://doi.org/10.1016/j.cell.2016.05.041

Levy, H., Raby, B. A., Lake, S., Tantisira, K. G., Kwiatkowski, D., Lazarus, R., … Weiss, S. T. (2005). Association of defensin β-1 gene polymorphisms with asthma. *The Journal of Allergy and Clinical Immunology*, *115*(2), 252–258. https://doi.org/10.1016/j.jaci.2004.11.013

Lilley, E., Stanford, S. C., Kendall, D. E., Alexander, S. P., Cirino, G., Docherty, J. R., George, C. H., Insel, P. A., Izzo, A. A., Ji, Y., Panettieri, R. A., Sobey, C. G., Stefanska, B., Stephens, G., Teixeira, M., & Ahluwalia, A. (2020). ARRIVE 2.0 and the *British Journal of Pharmacology*: Updated guidance for 2020. *British Journal of Pharmacology*. https://bpspubs.onlinelibrary.wiley.com/doi/full/10.1111/bph.15178

Ma, J., Rubin, B. K., & Voynow, J. A. (2018). Mucins, mucus, and goblet cells. *Chest*, *154*(1), 169–176. https://doi.org/10.1016/j.chest.2017.11.008

Madsen, J. M. (2001). Toxins as weapons of mass destruction. A comparison and contrast with biological-warfare and chemical-warfare agents. *Clinics in Laboratory Medicine*, *21*(3), 593-605. Retrieved from http://www.ncbi.nlm.nih.gov/pubmed/11577702

Matthay, M. A., Zemans, R. L., Zimmerman, G. A., Arabi, Y. M., Beitler, J. R., Mercat, A., … Calfee, C. S. (2019). Acute respiratory distress syndrome. *Nature Reviews. Disease Primers*, *5*(1), 18. https://doi.org/10.1038/s41572-019-0069-0

Mattix, M. E., Hunt, R. E., Wilhelmsen, C. L., Johnson, A. J., & Baze, W. B. (1995). Aerosolized staphylococcal enterotoxin B-induced pulmonary lesions in rhesus monkeys (*Macaca mulatta*). *Toxicologic Pathology*, *23*(3), 262–268. https://doi.org/10.1177/019262339502300304

McKallip, R. J., Lombard, C., Martin, B. R., Nagarkatti, M., & Nagarkatti, P. S. (2002). Δ^9-Tetrahydrocannabinol-induced apoptosis in the thymus and spleen as a mechanism of immunosuppression in vitro and in vivo. *The Journal of Pharmacology and Experimental Therapeutics*, *302*(2), 451–465. https://doi.org/10.1124/jpet.102.033506

Mohammed, A., Alghetaa, H., Sultan, M., Singh, N. P., Nagarkatti, P., & Nagarkatti, M. (2020). Administration of Δ9-tetrahydrocannabinol (THC) post-staphylococcal enterotoxin B exposure protects mice from acute respiratory distress syndrome and toxicity. *Frontiers in Pharmacology*, *11*(893), 14. https://doi.org/10.3389/fphar.2020.00893

Mokra, D., Mikolka, P., Kosutova, P., & Mokry, J. (2019). Corticosteroids in acute lung injury: The dilemma continues. *International Journal of Molecular Sciences*, *20*(19). https://doi.org/10.3390/ijms20194765

Nagarkatti, P., Pandey, R., Rieder, S. A., Hegde, V. L., & Nagarkatti, M. (2009). Cannabinoids as novel anti-inflammatory drugs. *Future Medicinal Chemistry*, *1*(7), 1333–1349. https://doi.org/10.4155/fmc.09.93

Nanchal, R. S., & Truwit, J. D. (2018). Recent advances in understanding and treating acute respiratory distress syndrome. *F1000Res*, *7*. https://doi.org/10.12688/f1000research.15493.1

Neamah, W. H., Singh, N. P., Alghetaa, H., Abdulla, O. A., Chatterjee, S., Busbee, P. B., … Nagarkatti, P. (2019). AhR activation leads to massive mobilization of myeloid-derived suppressor cells with immunosuppressive activity through regulation of CXCR2 and microRNA miR-150-5p and miR-543-3p that target anti-inflammatory genes. *Journal of Immunology*, *203*(7), 1830–1844. https://doi.org/10.4049/jimmunol.1900291

Oliver, W. T., & Wells, J. E. (2015). Lysozyme as an alternative to growth promoting antibiotics in swine production. *Journal of Animal Science and Biotechnology*, *6*(1), 35. https://doi.org/10.1186/s40104-015-0034-z

Ongey, E. L., Giessmann, R. T., Fons, M., Rappsilber, J., Adrian, L., & Neubauer, P. (2018). Heterologous biosynthesis, modifications and structural characterization of Ruminococcin-A, a lanthipeptide from the gut bacterium *Ruminococcus gnavus* E1, in *Escherichia coli*. *Frontiers in Microbiology*, *9*, 1688. https://doi.org/10.3389/fmicb.2018.01688

Pandey, R., Hegde, V. L., Nagarkatti, M., & Nagarkatti, P. S. (2011). Targeting cannabinoid receptors as a novel approach in the treatment of graft-versus-host disease: Evidence from an experimental murine model. *The Journal of Pharmacology and Experimental Therapeutics*, *338*(3), 819–828. https://doi.org/10.1124/jpet.111.182717

Percie du Sert, N., Hurst, V., Ahluwalia, A., Alam, S., Avey, M. T., Baker, M., … Würbel, H. (2020). The ARRIVE guidelines 2.0: Updated guidelines for reporting animal research. *PLoS Biology*, *18*(7), e3000410. https://doi.org/10.1371/journal.pbio.3000410

Rao, R., Nagarkatti, P. S., & Nagarkatti, M. (2015). Δ^9Tetrahydrocannabinol attenuates Staphylococcal enterotoxin B-induced inflammatory lung injury and prevents mortality in mice by modulation of miR-17-92 cluster and induction of T-regulatory cells. *British Journal of Pharmacology*, *172*(7), 1792–1806. https://doi.org/10.1111/bph.13026

Rieder, S. A., Chauhan, A., Singh, U., Nagarkatti, M., & Nagarkatti, P. (2010). Cannabinoid-induced apoptosis in immune cells as a pathway to immunosuppression. *Immunobiology*, *215*(8), 598–605. https://doi.org/10.1016/j.imbio.2009.04.001

Rios-Covian, D., Ruas-Madiedo, P., Margolles, A., Gueimonde, M., de Los Reyes-Gavilan, C. G., & Salazar, N. (2016). Intestinal short chain fatty acids and their link with diet and human health. *Frontiers in Microbiology*, *7*, 185. https://doi.org/10.3389/fmicb.2016.00185

Roy, M. G., Livraghi-Butrico, A., Fletcher, A. A., McElwee, M. M., Evans, S. E., Boerner, R. M., … Evans, C. M. (2014). Muc5b is required for airway defence. *Nature*, *505*(7483), 412–416. https://doi.org/10.1038/nature12807

Rubenfeld, G. D., & Herridge, M. S. (2007). Epidemiology and outcomes of acute lung injury. *Chest*, *131*(2), 554–562. https://doi.org/10.1378/chest.06-1976

Saeed, A. I., Rieder, S. A., Price, R. L., Barker, J., Nagarkatti, P., & Nagarkatti, M. (2012). Acute lung injury induced by Staphylococcal enterotoxin B: Disruption of terminal vessels as a mechanism of induction of vascular leak. *Microscopy and Microanalysis*, *18*(3), 445–452. https://doi.org/10.1017/S1431927612000190

Sarkar, S., Kimono, D., Albadrani, M., Seth, R. K., Busbee, P., Alghetaa, H., … Chatterjee, S. (2019). Environmental microcystin targets the microbiome and increases the risk of intestinal inflammatory pathology via NOX2 in underlying murine model of nonalcoholic fatty liver disease. *Scientific Reports*, *9*(1), 8742. https://doi.org/10.1038/s41598-019-45009-1

Segata, N., Izard, J., Waldron, L., Gevers, D., Miropolsky, L., Garrett, W. S., & Huttenhower, C. (2011). Metagenomic biomarker discovery and explanation. *Genome Biology*, *12*(6), R60. https://doi.org/10.1186/gb-2011-12-6-r60

Shu, Q., Shi, Z., Zhao, Z., Chen, Z., Yao, H., Chen, Q., … Fang, X. (2006). Protection against *Pseudomonas aeruginosa* pneumonia and sepsis-induced lung injury by overexpression of β-defensin-2 in rats. *Shock*, *26*(4), 365–371. https://doi.org/10.1097/01.shk.0000224722.65929.58

Sido, J. M., Jackson, A. R., Nagarkatti, P. S., & Nagarkatti, M. (2016). Marijuana-derived Δ-9-tetrahydrocannabinol suppresses Th1/Th17 cell-mediated delayed-type hypersensitivity through microRNA regulation. *Journal of Molecular Medicine (Berlin, Germany)*, *94*(9), 1039–1051. https://doi.org/10.1007/s00109-016-1404-5

Sido, J. M., Nagarkatti, P. S., & Nagarkatti, M. (2015). Δ^9-Tetrahydrocannabinol attenuates allogeneic host-versus-graft response and delays skin graft rejection through activation of cannabinoid receptor 1 and induction of myeloid-derived suppressor cells. *Journal of Leukocyte Biology*, *98*(3), 435–447. https://doi.org/10.1189/jlb.3A0115-030RR

Tauxe, W. M., Dhere, T., Ward, A., Racsa, L. D., Varkey, J. B., & Kraft, C. S. (2015). Fecal microbiota transplant protocol for clostridium difficile infection. *Laboratoriums Medizin*, *46*(1), e19–e23. https://doi.org/10.1309/LMCI95M0TWPDZKOD

Van Gelder, R. N., von Zastrow, M. E., Yool, A., Dement, W. C., Barchas, J. D., & Eberwine, J. H. (1990). Amplified RNA synthesized from limited quantities of heterogeneous cDNA. *Proceedings of the National Academy of Sciences of the United States of America*, *87*(5), 1663–1667. Retrieved. from, https://www.ncbi.nlm.nih.gov/pubmed/1689846

Vaughan, A. E., Brumwell, A. N., Xi, Y., Gotts, J. E., Brownfield, D. G., Treutlein, B., … Chapman, H. A. (2015). Lineage-negative progenitors mobilize to regenerate lung epithelium after major injury. *Nature*, *517*(7536), 621–625. https://doi.org/10.1038/nature14112

Vinolo, M. A., Rodrigues, H. G., Nachbar, R. T., & Curi, R. (2011). Regulation of inflammation by short chain fatty acids. *Nutrients*, *3*(10), 858–876. https://doi.org/10.3390/nu3100858

Weber, N., Liou, D., Dommer, J., MacMenamin, P., Quiñones, M., Misner, I., … Ezeji, S. (2018). Nephele: A cloud platform for simplified, standardized and reproducible microbiome data analysis. *Bioinformatics*, *34*(8), 1411–1413. https://doi.org/10.1093/bioinformatics/btx617

Yang, X., Hegde, V. L., Rao, R., Zhang, J., Nagarkatti, P. S., & Nagarkatti, M. (2014). Histone modifications are associated with Δ^9-tetrahydrocannabinol-mediated alterations in antigen-specific T cell responses. *The Journal of Biological Chemistry*, *289*(27), 18707–18718. https://doi.org/10.1074/jbc.M113.545210

Zambon, M., & Vincent, J. L. (2008). Mortality rates for patients with acute lung injury/ARDS have decreased over time. *Chest*, *133*(5), 1120–1127. https://doi.org/10.1378/chest.07-2134

Zgair, A., Lee, J. B., Wong, J. C., Taha, D. A., Aram, J., Di Virgilio, D., … Fischer, P. M. (2017). Oral administration of cannabis with lipids leads to high levels of cannabinoids in the intestinal lymphatic system and prominent immunomodulation. *Scientific Reports*, *7*(1), 14542. https://doi.org/10.1038/s41598-017-15026-z

SUPPORTING INFORMATION

Additional supporting information may be found online in the Supporting Information section at the end of this article.

How to cite this article: Mohammed A, Alghetaa HK, Zhou J, Chatterjee S, Nagarkatti P, Nagarkatti M. Protective effects of Δ^9-tetrahydrocannabinol against enterotoxin-induced acute respiratory distress syndrome are mediated by modulation of microbiota. *Br J Pharmacol*. 2020;177:5078–5095. https://doi.org/10.1111/bph.15226